Chemistry of new particle growth in mixed urban and biogenic emissions - Insights from CARES

A. Setyan[1,*], C. Song[2], M. Merkel[3], W. B. Knighton[4], T. B. Onasch[5], M. R. Canagaratna[5], D. R. Worsnop[5,6], A. Wiedensohler[3], J. E. Shilling[2], Q. Zhang[1,#]

[1] Department of Environmental Toxicology, 1 Shields Ave., University of California, Davis, CA 95616, United States

[2] Atmospheric Sciences and Global Change Division, Pacific Northwest National Laboratory, Richmond, WA 99352, United States

[3] Leibniz Institute for Tropospheric Research, 04318 Leipzig, Germany

[4] Montana State University, Bozeman, MT 59717, United States

[5] Aerodyne Research Inc., Billerica, MA 01821, United States

[6] Department of Physics, University of Helsinki, FI-00014 Helsinki, Finland

[*] Now at: Empa, Swiss Federal Laboratories for Materials Science and Technology, 8600 Dübendorf, Switzerland

[#] Correspondence to: Qi Zhang (dkwzhang@ucdavis.edu; phone #: 530-752-5779)

In preparation for

Atmospheric Chemistry and Physics

Special issue: Carbonaceous Aerosols and Radiative Effects Study (CARES)

Abstract

Regional new particle formation and growth events (NPE) were observed on most days over the Sacramento and western Sierra Foothills area of California in June 2010 during the Carbonaceous Aerosols and Radiative Effect Study (CARES). Simultaneous particle measurements at both the T0 (Sacramento, urban site) and the T1 (Cool, rural site located ~40 km northeast of Sacramento) sites of CARES indicate that the NPE usually occurred in the morning with the appearance of an ultrafine mode at ~15 nm (in mobility diameter, D_m, measured by a mobility particle size spectrometer operating in the range 10-858 nm) followed by the growth of this modal diameter to ~50 nm in the afternoon. These events were generally associated with southwesterly winds bringing urban plumes from Sacramento to the T1 site. The growth rate was on average higher at T0 (7.1±2.7 nm/hr) than at T1 (6.2±2.5 nm/hr), likely due to stronger anthropogenic influences at T0. Using a high-resolution time-of-flight aerosol mass spectrometer (HR-ToF-AMS), we investigated the evolution of the size-resolved chemical composition of new particles at T1. Our results indicate that the growth of new particles was driven primarily by the condensation of oxygenated organic species and, to a lesser extent, ammonium sulfate. New particles appear to be fully neutralized during growth, consistent with high NH_3 concentration in the region. Nitrogen-containing organic ions (i.e., CHN^+, CH_4N^+, $C_2H_3N^+$, and $C_2H_4N^+$) that are indicative of the presence of alkyl-amine species in submicrometer particles enhanced significantly during the NPE days, suggesting that amines might have played a role in these events. Our results also indicate that the bulk composition of the ultrafine mode organics during NPE was very similar to that of anthropogenically-influenced secondary organic aerosol (SOA) observed in transported urban plumes. In addition, the concentrations of species representative of urban emissions (e.g., black carbon, CO, NO_x, and toluene) were significantly higher whereas the photo-oxidation products of biogenic VOC and the biogenically-influenced SOA also increased moderately during the NPE days compared to the non-event days. These results indicate that the frequently occurring NPE over the Sacramento and Sierra Nevada regions were mainly driven by urban plumes from Sacramento and the San Francisco Bay Area and that the interaction of regional biogenic emissions with the urban

plumes has enhanced the new particle growth. This finding has important implication for quantifying the climate impacts of NPE on global scale.

1 Introduction

New particle formation and growth processes are an important source of ultrafine particles in both clean and polluted environments. A large number of studies reported the observations of intensive new particle events at various locations, including urban areas (e.g., Brock et al., 2003; Dunn et al., 2004; Stanier et al., 2004; Zhang et al., 2004a; Wu et al., 2007; Ahlm et al., 2012), remote sites (e.g., Weber et al., 1999; Creamean et al., 2011; Vakkari et al., 2011; Pikridas et al., 2012), forested locations (e.g., Allan et al., 2006; Pierce et al., 2012; Han et al., 2013), coastal sites (e.g., O'Dowd et al., 2002; Wen et al., 2006; Liu et al., 2008; Modini et al., 2009), and polar regions (e.g., Komppula et al., 2003; Koponen et al., 2003; Asmi et al., 2010). These events significantly affect the number concentrations and size distributions of particles in the atmosphere with important implications on human health and climate (Spracklen et al., 2006; Bzdek and Johnston, 2010; Kerminen et al., 2012). However, despite frequent observations, the chemical processes underlying the formation and growth of new particles remain poorly understood.

New particle events occur in two steps, i.e., the formation of nuclei, followed by the growth of the stable clusters to larger sizes by condensation of low-volatility compounds and coagulation. For ambient measurements, the evolution of the number-based particle size distribution is a main criterion for identifying the onset of new particle events. Mobility particle size spectrometer (MPSS), also called scanning mobility particle sizer (SMPS), is the most widely used instrument to determine the particle number concentration and size distribution during these events. The evolution of the chemical composition of ultrafine particles during new particle formation and growth is another piece of critical information needed for understanding this process. For that purpose, aerosol mass spectrometer (AMS) (e.g., Zhang et al., 2004a; Allan et al., 2006; Ziemba et al., 2010; Creamean et al., 2011; Ahlm et al., 2012), chemical ionization mass spectrometer (CIMS) (e.g., Dunn et al., 2004; Smith et al., 2005; Smith et al., 2008; Smith et al., 2010; Jokinen et al., 2012), Nano aerosol mass spectrometer (NAMS) (e.g., Bzdek et al., 2011; Bzdek et al., 2012), and atmospheric pressure ionization time-of-flight (APi-TOF) mass spectrometer (Lehtipalo et al., 2011; Kulmala et al., 2013) have been successfully deployed in the field to study the chemical processes underlying atmospheric new particle events.

An important finding from previous studies is that organics and sulfates are usually involved in the growth of new particles up to sizes where they can act as cloud condensation nuclei (CCN). The contribution of these two species to particle growth depends on the concentrations of the precursors and meteorological conditions. For example, at urban or industrial locations where the SO_2 mixing ratio is high, sulfate is an important contributor to the growth of new particles (Brock et al., 2003; Zhang et al., 2004a; Yue et al., 2010; Bzdek et al., 2012). At rural and remote locations, however, the growth of new particles was found to be almost exclusively driven by organics (Smith et al., 2008; Laaksonen et al., 2008; Ziemba et al., 2010; Pierce et al., 2012; Ahlm et al., 2012). In addition, it was found that in Pittsburgh, USA, despite high ambient SO_2 concentrations, H_2SO_4 contributes mainly to the early stage of the new particle growth, while the growth up to CCN sizes is mainly driven by secondary organic aerosols (SOA), especially during late morning and afternoon when photochemistry is more intense (Zhang et al., 2004a; Zhang et al., 2005).

SOA is a major component of fine particles globally (Zhang et al., 2007; Jimenez et al., 2009). Understanding its roles in new particle formation and growth is important for addressing aerosols' effects on climate and human health. Recent studies found significantly enhanced SOA formation rates in mixed biogenic and anthropogenic emissions (de Gouw et al., 2005; Volkamer et al., 2006; Kleinman et al., 2008; Setyan et al., 2012; Shilling et al., 2013). However, there is little known about the influence of the interactions of organic species from biogenic and anthropogenic sources on new particle growth. The Sacramento Valley in California is a place of choice to study this process. The Sacramento metropolitan area lies in the Central Valley to the north of the San Joaquin River Delta and to the southwest of the forested Sierra Nevada Mountains. The wind in this region is characterized by a very regular pattern, especially in summer (Fast et al., 2012). Indeed, during the day, a southwesterly wind usually brings air masses from the San Francisco Bay to the Sacramento metropolitan area and pushes northeast to the Sierra Nevada Mountains (Dillon et al., 2002), promoting the transport of urban plumes from Sacramento to forested regions where biogenic emissions are intense.

The U.S. Department of Energy (DOE) sponsored Carbonaceous Aerosols and Radiative Effects Study (CARES) that took place in the Sacramento Valley in June 2010 was designed to

take advantage of this regular wind pattern to better understand the life-cycle processes and radiative properties of carbonaceous aerosols in a region influenced by both anthropogenic and biogenic emissions (Zaveri et al., 2012). Within the framework of CARES, a wide range of instruments were deployed between June 2 and 28, 2010 at two ground sites located in Sacramento (T0, urban site) and Cool, CA at the foothills of the Sierra Nevada Mountains (T1, rural site), respectively, to measure size-resolved chemical compositions, number size distributions, and optical and hygroscopic properties of aerosols, as well as trace gases and meteorological data (Zaveri et al., 2012). One of the major observations during CARES was that particles were dominated by organics in this region, and that the formation of SOA was enhanced when anthropogenic emissions from the Sacramento metropolitan area and the Bay Area were transported to the foothills and mixed with biogenic emissions (Setyan et al., 2012; Shilling et al., 2013).

During CARES, new particle growth events were observed almost daily at both the T0 and T1 sites. Similarly, previous studies conducted at the University of California Blodgett Forest Research Station, approximately 75 km to the northeast of Sacramento and 35 km to the northeast of the T1 site, also reported the frequent occurrence of NPE (Lunden et al., 2006; Creamean et al., 2011). In their study conducted from May to September 2002, Lunden et al. (2006) found that the oxidation products of reactive biogenic compounds accounted for a significant portion of the particle growth. The study of Creamean et al. (2011), which took place in early spring of 2009, found that sulfates and amines participated in the growth of new particles and that long-range transport of SO_2 from Asia seemed to contribute to faster growth. These findings indicate that new particle formation and growth are important processes in Northern California and are affected by regional anthropogenic and biogenic emissions as well as by pollutants transported from Asia. Understanding to what extent these emissions may govern the NPE's requires measurements of size-resolved chemical compositions of the new particles. The main aim of the present paper is to examine the evolution characteristics of new particles at the T0 and T1 sites during CARES, with a focus on the evolution of size-resolved particle chemical composition based on HR-ToF-AMS measurements at T1.

2 Experimental

2.1 Sampling site and instrumentation

The T0 sampling site was located on the campus of the American River College in Sacramento (38° 39′ 01” N, 121° 20′ 49” W, 30 m above sea level) and the T1 site was located on the campus of the Northside School at Cool (38° 52′ 16” N, 121° 01′ 22” W, 450 m above sea level). Sacramento is the capital of California, with 480,000 inhabitants in the city and 2.5 million people living in the metropolitan area. Cool is a small town (2500 inhabitants) surrounded by very large forested areas, and located ~40 km northeast of Sacramento at the Sierra Nevada foothills.

In this paper, we report results of particle chemical compositions at T1, and particle number size distributions at both T0 and T1. Size-resolved chemical composition of non-refractory submicron aerosols (NR-PM_1) were measured at T1 using an Aerodyne HR-AMS (DeCarlo et al., 2006; Canagaratna et al., 2007). A detailed discussion on its operation during the present study was presented in Setyan et al. (2012). Briefly, the HR-AMS was equipped with a standard aerodynamic lens, described in Zhang et al. (2004b), and allowing the transmission of particles in the range ~30-1500 nm (in vacuum aerodynamic diameter, D_{va}). The instrument was operated alternatively in V- and W-mode every 2.5 min. In V-mode, data was recorded in mass spectrum (MS) mode and particle time-of-flight (PToF) mode. The MS mode was used to obtain average mass spectra and determine the concentration of the species in submicrometer particles without size information. In the PToF mode, average mass spectra were acquired for 92 size bins covering 30-1500 nm (D_{va}), allowing the determination of the size-resolved chemical composition. W-mode data was recorded exclusively in MS mode.

The particle number size distribution was measured both at T0 and T1 with a MPSS (also called SMPS) as described in Wiedensohler et al. (2012). The instrument used at T1 consists of a Hauke-type differential mobility analyzer (DMA) and a condensation particle counter (CPC; TSI Inc., Shoreview, MN; model 3772), and used ^{210}Po as radioactive source for the neutralizer (Setyan et al., 2012). The MPSS was set to measure particles in the range 10-858 nm (in mobility diameter, D_m), divided into 70 logarithmically distributed size bins. MPSS data has been corrected to take into account the DMA-CPC lag time, bipolar charge distribution, CPC

efficiency, and diffusion loss. The SMPS deployed at T0 was a commercial instrument (TSI Inc.; model 3936), and was constituted of a ^{85}Kr neutralizer, a DMA (TSI Inc.; model 3080 with the long column) and a CPC (TSI Inc.; model 3775). The instrument measured particles in the size range of 12-737 nm (in D_m) divided into 115 size bins. Diffusion loss correction was applied after the data inversion. All dates and times reported in this paper are in Pacific Daylight Time (PDT = UTC – 7 hr), which was the local time during this study.

2.2 Data analysis

Particle number concentration and size distribution have been used to identify new particle events in the atmosphere. However, given that the new particles formed by nucleation have generally a diameter in the size range 1-3 nm, smaller than the smallest size measured by our MPSS's, we were not able to observe the new particle formation themselves during the present study, but only the growth of the newly formed particles that are larger than 10 nm. For this reason, we will not use the terms "nucleation" or "new particle formation" in the forthcoming discussion, but rather "new particle growth". Each day for which complete MPSS data was available was classified as new particle event (NPE) day if the particle number concentration in the size range 12-20 nm increased by more than 800 particles/cm^3, and if this increase was accompanied by the increase of the modal diameter during the following hours. These two conditions allowed us to distinguish NPE from primary emissions from vehicles, which also produce small particles but are usually observed as occasional spikes in the time series of the particle number concentration in the range 12-20 nm. In addition, each growth event was considered as "strong" if the increase of the particle number concentration in the range 12-20 nm was higher than 1500 particles/cm^3, and "weak" if the increase was lower than this threshold. A summary of the new particle growth events observed during this study is provided in Table 1.

The modal diameter(s) of each particle number size distribution recorded during this study have been determined with a multiple peak fitting tool available in Igor Pro 6.2.2.2 (WaveMetrics Inc., Lake Oswego, OR). All the size distributions were log normal. The growth rate (GR), which corresponds to the increase of the modal diameter of newly formed particles per time unit (nm/hr), has been calculated for each individual growth event using Equation 1:

$$GR = \frac{\Delta Dm}{\Delta t} \quad (1)$$

in which ΔD_m is the difference of the modal diameter (nm) between the beginning of the growth and the period when the growth significantly slows down, and Δt is the duration of the growth (hr).

3 Results and discussions

3.1 Evolution of particle number size distributions during regional new particle events

The SMPS and MPSS were fully operational during 26 days at T0, and 22 days at T1, from June 2 – 29, 2010. The time series of the particle number size distributions show that new particle events frequently occurred at both sites (Fig. 1), indicating that these events occurred on a regional scale. A total of 19 NPE were identified at T1 (86% of the time; Table 1), eight of which were considered as "strong" and eleven as "weak". Most of the events (14 in total) occurred during periods of southwesterly wind that transported urban plumes to the T1 site (i.e., T0 → T1), except for 5 events which occurred during northwesterly wind periods (Table 1). In addition, all 8 strong NPE occurred during the T0 → T1 periods (Table 1). At T0, 22 new particle events were identified, 18 of which were considered as "strong" and only four events were "weak".

Fig. 2 compares the average daily evolution patterns of particle number concentrations at the T0 and T1 sites during NPE days. Generally, the increase of the particle number concentration during these events was significantly higher at T0 than at T1 (average $9.6 \cdot 10^3$ vs. $3.8 \cdot 10^3$ #/cm^3/hr, $p<0.05$ with Student's t-test; Table 1). The average ($\pm 1\sigma$) growth rate of new particles was also higher at T0 (7.1 ± 2.7 nm/hr vs. 6.2 ± 2.5 nm/hr at T1), but the difference was not statistically significant (i.e., $p>0.05$ with Student's t-test). The growth rates given in Table 1 correspond to the first hours of the observation, when the increase of the modal diameter is linear. Indeed, the growth rate is usually quite linear during the first 2-3 hours and slows down afterwards (Fig. 5a and 5c). One reason for the decrease of the growth rate after a few hours may be due to the fact that when particles grow to a certain diameter, the condensation of additional species onto the surface of these particles will result in a very small increase of their sizes. The occurrence of relatively stronger NPE at T0 is likely due to the proximity of emission sources of precursor species and a higher anthropogenic influence. Indeed, the frequency as well as the

228 growth rates observed during the present study were much higher than those reported by Lunden
229 et al. (2006) at ~35 km northeast of T1 (frequency = 30% of the time, average growth rate = 3.8
230 ± 1.9 nm/hr), where the lower frequency and growth rates might be related to the fact that their
231 site was located deeper into the forest and subjected to relatively lesser anthropogenic influences
232 from urban areas to the southwest (e.g., Sacramento and the San Francisco Bay Area). The
233 growth rates measured during the present study are also much higher than those observed at
234 Hyytiälä, Finland, where NPE have been extensively observed and described over the past 15
235 years. Riipinen et al. (2011) report a median growth rate of 2.3 nm/hr during the years 2003-
236 2007, much lower than at T1 (6.2 nm/hr) and T0 (7.1 nm/hr). NPE at Hyytiälä are mainly driven
237 by the photooxidation of biogenic precursors, and thus growth rates measured in this kind of
238 environment depend on the concentration and volatility of the condensing material (Pierce et al.,
239 2011; Riipinen et al., 2011; Pierce et al., 2012; Riipinen et al., 2012). The Sacramento and Sierra
240 Foothill region, however, is influenced by both urban and biogenic emission sources. Thus, the
241 comparison between the growth rates at these different sites suggests that the degree of
242 anthropogenic influence may be an important factor driving the growth rate.
243 During the present study, all growth events began in the morning, with the appearance of an
244 Aitken mode observed with the MPSS between 9:00 and 12:00 (PDT). Particle growth lasted
245 several hours, with size modes reaching their maximum in the afternoon, typically after 15:00.
246 The modal diameters at the end of the growth in general peaked between 40-50 nm, but for
247 several cases, the modal diameter did not reach 35 nm, especially for the weakest events or when
248 a change in the wind direction was observed during the day (Fig. 1).
249 An important observation of the present study is that NPE began at T1 a few hours later than
250 at T0, especially during days characterized with daytime T0 → T1 transport. A typical example
251 of this phenomenon occurred on June 26 (Fig. 3 and 4). According to Fast et al. (2012) , a T0 to
252 T1 transport occurred that day. Particles smaller than 20 nm (in D_m) began to increase slightly
253 before 9:00 at T0 (Fig. 3a), and an Aitken mode appeared at the same time (Fig. 4). Then, during
254 the following hours, the modal diameter increased slowly up to ~50 nm (in D_m), likely due to
255 condensation of low-volatility compounds onto the surface of these new particles. The increase
256 of the modal diameter could also be due to coagulation, but this process is expected to be very

slow for particles in the Aitken mode. Thus, as shown in Fig. 3a, the evolution of the particle number size distribution shows a "banana shape", which is a typical observation for the growth of new particles. At T1, the same phenomenon occurred at ~11:00, i.e., 2 hours after T0 (Fig. 3b). This time delay is consistent with the wind data recorded at T1 which indicate the sampling of air masses transported from the T0 direction. The much lower concentrations of particles smaller than 20 nm between 9:00 and 11:00 at T1 (Fig. 3b), compared with T0 (Fig. 3a), suggests that new particle formation occurred much near and upwind of T0 and not close to T1. In other words, the banana-shaped evolution pattern observed at T1 was likely independent of the emissions in the T1 area and mostly dependent on the emissions near T0 and upwind of T0. Further evidence for this pseudo Lagrangian sampling is the observation of a sudden change in wind direction at ~14:30 at T0 that brought in a very clean air mass associated with a sharp decrease of particle number concentration that lasted for ~3.5 hours (Fig. 3a). Particle concentration at T0 increased again at ~18:00 after a shift of the wind direction back to southwesterly. A mirrored decrease of particle concentration, although less dramatically, was observed at 16:30 at T1, ~2 hours after the clean air mass event at T0 (Fig. 3b). The increase of particle number concentration occurred at T1 around 21:00, ~3 hours after the increase occurred at T1, consistent with gradually decreasing wind speed from 16:30 to 21:00. The wind direction at T1 remained southwesterly during the entire afternoon (Fig. 3b).

This time delay between T0 and T1 was also observed during the other events, and this is confirmed by the diurnal evolution profiles of particle number concentrations (Fig. 2) and size distributions at both sites (Fig. 5a and 5c). These observations indicate that new particle growth generally occurred during T0 → T1 transport promoted by the daytime southwesterly wind and that the new particle growth events were generally more intense at T0 compared to at T1. Wind rose plot during NPE (Fig. 6g) confirms that these events usually occurred when the wind was coming from the southwest, which corresponds to the location of the Sacramento metropolitan area. On the other hand, when NPE was not observed, the wind was coming mainly from the northwest and the west (Fig. 6h), bringing air masses dominated by biogenic emissions (Setyan et al., 2012), thus reducing anthropogenic influences at T1.

It is interesting to notice that the evolution of the particle number size distributions and concentrations during the evening and the night is not similar at T0 and T1. At T0, particle number concentration remains almost constant between 23:00 and 8:00, while the mode is centered at ~35-40 nm (in D_m) during this period (Fig. 5a). On the contrary, particle number concentration decreases gradually at T1 during night, while the modal diameter increases from 35 nm (at 21:00) up to 90 nm (at 14:00 the following day; Fig. 5c). This may be due to the fact that the T0 site was more influenced by nanoparticles from vehicular emissions than the T1 site, due to the proximity of traffic, anthropogenic emissions, and transport from the Bay Area. On the other hand, the T1 site was more influenced by downslope winds during the night, when a change in the wind direction brought down more aged aerosols from the Sierra Nevada to the foothills (Setyan et al., 2012).

3.2 Evolution of particle chemistry during new particle growth

The evolution of particle chemistry during NPE at T1 was studied in detail with a HR-ToF-AMS. As summarized in Table 1, the increase of particle number concentration during the new particle growth events was accompanied by an increase of organics and sulfate in ultrafine particles (40-120 nm in D_{va}). The average (± 1σ) increase of organics in that size range was 0.71 (± 0.29) μg/m^3 while that of sulfate was 0.10 (± 0.11) μg/m^3.

Fig. 6 shows the diurnal size distributions of organic matter, sulfate, and particle volume concentrations, along with the wind rose plots during NPE days and non-event days. The growth of new particles was mainly contributed by sulfate and organics (Fig. 6a and 6c), but the increase of particle mass observed by the AMS occurred after 11:00, later than the increase of number concentration according to the SPMS. This is because the smallest size measured by our MPSS is 10 nm (in D_m), while the transmission through the AMS is significant only for particles larger than 30 nm (in D_{va}) (Jayne et al., 2000). Given that particle density at T1 was on average 1.4 during this study (Setyan et al., 2012), and assuming that they are spherical, the smallest particles measured by the AMS correspond to ~21 nm in D_m. Thus, the MPSS was the first instrument to detect the growth of new particles, while the HR-ToF-AMS observed the growth 2 or 3 hours later, depending on the growth rate. A similar observation was reported during NPE in Pittsburgh (Zhang et al., 2004a). It is interesting to notice that organics, sulfate, and particle volume exhibit

qualitatively the same diurnal size distributions (Fig. 6). Indeed, they have a constant modal diameter in larger particles during the entire day, and they increase in ultrafine particles in the afternoon during the growth events.

The diurnal patterns of organics and sulfate in three different size ranges (40-120, 120-200, and 200-800 nm in D_{va}) show that their afternoon increase occurred mainly in ultrafine particles (40-120 nm) while the increases in the rest of the sizes were moderate during NPE days (Fig. 7a and 7c). In comparison, the diurnal profiles of both species were relatively flat and their concentrations much lower during the non-event days (Fig. 7b and 7d). Although both organics and sulfate in ultrafine particles increased in the afternoon, the increase of the organic mass in the 40-120 nm particles was on average 7 times higher than that of sulfate (see above and Fig. 8d and 8e). Clearly, the growth of new particles was mainly driven by organics. This is in agreement with previous studies, which also emphasized the key-role of organics in the growth of new particles up to CCN sizes (Laaksonen et al., 2008; Smith et al., 2008; Ziemba et al., 2010; Zhang et al., 2011; Ahlm et al., 2012; Pierce et al., 2012; Riipinen et al., 2012).

Another important observation is the substantial increase of the signals of four nitrogen-containing ions (i.e., CHN^+, CH_4N^+, $C_2H_3N^+$, and $C_2H_4N^+$) in submicron particles during the new particle growth periods (Fig. 8f). On average, the concentration of these ions during NPE days was 2.4 times the concentration observed during non-NPE days (Fig. 11). Since these $C_xH_yN^+$ ions are generally related to alkyl-amine species (Ge et al., 2014), this class of compounds was likely involved in the growth of new particles. This is consistent with previous findings in the atmosphere (e.g., Makela et al., 2001; Smith et al., 2008; Smith et al., 2010; Bzdek et al., 2011; Creamean et al., 2011; Laitinen et al., 2011). Recent studies have found that sulfuric acid–amine clusters are highly stable and that even trace amount of amines (e.g., a few ppt) can enhance particle formation rates by orders of magnitude compared with ammonia (Zollner et al., 2012; Almeida et al., 2013). The importance of gas-phase amines in the generation of organic salts involved in the formation of new particles was also confirmed by thermodynamic modeling study (Barsanti et al., 2009). Based on the mass spectrometry fragmentation patterns of amine standards analyzed in our lab (Ge et al., in preparation), the average concentration of aminium ($R_1R_2R_3N^+$, where R_1, R_2, R_3 are either H or an alkyl group) is estimated to be approximately

343 1/10th that of ammonium at T1 during this study (Fig. 8f). Although we are unable to directly
344 assess the importance of amines in new particle formation based on this study, our results
345 suggest that amines likely played an important role in the formation of new particles in the
346 Sacramento and Sierra foothills region.
347 Due to the high contribution of organics to submicron aerosol mass in the region, positive
348 matrix factorization (PMF) analysis was performed on the high resolution mass spectra of the
349 AMS to investigate the sources and processes of organic aerosols (Setyan et al., 2012). Briefly,
350 three distinct factors were determined, including a biogenically-influenced SOA associated with
351 the regional biogenic emissions (O/C ratio = 0.54, 40% of total organic mass), an
352 anthropogenically-influenced SOA associated with transported urban plumes (O/C ratio = 0.42,
353 51%), and a hydrocarbon-like organic aerosol (HOA) mainly associated with local primary
354 emissions (O/C ratio = 0.08, 9%). Details on the determination and validation of these three OA
355 types are given in Setyan et al. (2012). It is important to clarify here that the biogenic SOA and
356 urban transport SOA identified at T1 do not correspond to SOAs formed from 100%
357 anthropogenic or biogenic precursors. In fact, the so-called biogenic SOA was found in air
358 masses with dominant biogenic influence and little anthropogenic influence, while the urban
359 transport SOA was found in air masses characterized as urban plumes mixed with the
360 continuously present biogenic emissions in the region. These observations are consistent with
361 radiocarbon analysis of fine particulate matter, which has shown that modern carbon worldwide
362 often contributes > 70% of the total carbon, particularly downwind of urban areas (Glasius et al.,
363 2011;Schichtel et al., 2008 and references therein).
364 As shown in Fig. 8, during NPE days, the mass concentration of urban transport SOA
365 increased by more than a factor of 2 (from 0.75 to 1.7 μg/m^3) between 10:00 and 16:00 (Fig. 8b),
366 whereas that of biogenic SOA increased only slightly by ~ 10% during that period (from 0.84 –
367 0.93 μg/m^3, Fig. 8c). This result underlines the key-role played by the urban plumes from
368 Sacramento in the NPEs at Sierra foothills.
369 Fig. 9 shows the evolutions of the mass-weighted size distributions of Org, SO_4^{2-}, organic
370 tracer ions, and particle number distributions during daytime. The average size distributions of
371 Org and SO_4^{2-} during NPE days show significant increase of concentrations in the small mode

372 (Fig. 9e and 9g). On the other hand, the increases of the concentrations of Org and SO_4^{2-} in
373 ultrafine particles were all negligible during non-event days (Fig. 9f and 9h).
374 Another important parameter to determine was the neutralization of sulfate in the ultrafine
375 mode during NPE. We already know from the mass spectral mode of the AMS that sulfate was
376 fully neutralized in the bulk during the entire study (Setyan et al., 2012). Many previous studies
377 mentioned that sulfate involved in NPE was usually under the form of sulfuric acid, especially
378 during the initial steps of the growth (Brock et al., 2003; Zhang et al., 2004a; Yue et al., 2010;
379 Bzdek et al., 2012). However, northern California contains very large agricultural regions with a
380 lot of sources of ammonia, which could possibly neutralize sulfate in the ultrafine mode. Using
381 high mass resolution mass spectra acquired under PToF mode, we determined the size
382 distributions of ammonium and sulfate based on those of the NH_3^+ and SO^+, which are the ions
383 of ammonium and sulfate, respectively, with the highest signal-to-noise ratio (see supplementary
384 material for details of this data treatment). As shown in Fig. 10, despite relatively noisy data, the
385 size distributions suggest that sulfate was fully neutralized by ammonium in the entire size range,
386 including ultrafine particles. Moreover, we did not observe any difference in the sulfate
387 neutralization between NPE and non-NPE days or between different times of the day. These
388 results indicate that sulfate in ultrafine particles was present in the form of ammonium sulfate
389 and that sulfuric acid was quickly neutralized after condensation.

390 ### 3.3 Anthropogenic influence on new particle growth events

391 The average concentrations and diurnal patterns of VOCs, trace gases (O_3, CO, NO_x), BC,
392 and meteorological parameters (temperature, relative humidity, and solar radiation) during NPE
393 days and non-event days were compared (Fig. 11, Fig. S3 and S4, and Table 2). An important
394 difference between NPE and non-event days was the concentrations of photo-oxidation products
395 (formaldehyde and acetaldehyde) and anthropogenic precursors (BC, CO and toluene), which
396 were all significantly higher during NPE days than during non-event days. Photo-oxidation
397 products were on average ~50% more concentrated on NPE days (formaldehyde: 2.71 ± 1.39 ppb
398 vs. 1.83 ± 0.81 ppb during non-NPE days; acetaldehyde: 0.97 ± 0.47 ppb vs. 0.71 ± 0.24 ppb).
399 The sum of methacrolein (MACR) and methyl vinyl ketone (MVK), which are the first
400 generational products of isoprene oxidation, was also ~20% higher during NPE days: 0.98 ± 0.79

401 ppb vs. 0.75 ± 0.50 ppb. These markers of oxidation are likely correlated with other semi-volatile
402 compounds co-generated during photo-oxidation, which could condense onto the surface of
403 particles and could be an important factor driving the growth of new particles. Moreover, the
404 diurnal patterns of these compounds during NPE and non-NPE days show a clear difference
405 during the afternoon, whereas the differences are much smaller during nighttime (Fig. S4). This
406 result stresses the influence of photochemistry on the formation and growth of new particles.
407 The average concentrations of isoprene were almost identical during NPE and non-event
408 days (Fig. 11) but the enhancements of anthropogenic species during NPE days were more
409 dramatic. The average concentrations of BC (0.042 ± 0.028 μg m^{-3} during NPE days vs. 0.027 ±
410 0.017 μg m^{-3} during non-NPE days), CO (130 ± 27.0 vs. 99.8 ± 19.8 ppb), NO_x (3.8 ± 3.3 vs. 2.7
411 ± 3.5 ppb), HOA (0.16 ± 0.15 vs. 0.11 ± 0.08 μg m^{-3}), and toluene (0.060 ± 0.037 vs. 0.038 ±
412 0.019 ppb; Table 2) were 30-60% higher on NPE days. According to the Student's t-test, the
413 difference between NPE and non-NPE days was significant (i.e., $p<0.05$) for all the
414 anthropogenic species, except for NO_x. The ozone concentrations, however, were very similar
415 between two types of days (46.2 ± 10.5 ppb during non-NPE vs. 43.5 ± 14.2 ppb). These results
416 point out the importance of the anthropogenic influence on the formation and growth of new
417 particles. However, during a study undertaken at the Blodgett Forest, which is located ~35 km on
418 the northeast of the present sampling site and ~75 km downwind from Sacramento, Lunden et al.
419 (2006) observed new particle growth events when the degree of anthropogenic influence was
420 significantly reduced.
421 The relative humidity (RH) was higher on NPE days (45 ± 13 %) compared to non-NPE days
422 (27 ± 12 %). Previous studies, however, found contradictory links between NPEs and RH. For
423 example, Lunden et al. (2006) and Charron et al. (2007) observed much higher RH during NPEs
424 days than non-NPE days. In addition, most of the previous studies reported NPEs when the RH
425 was low (Boy and Kulmala, 2002; Hamed et al., 2007; Jeong et al., 2010; Hamed et al., 2011;
426 Guo et al., 2012). The exact role of RH in NPEs is not clearly elucidated yet. According to
427 Hamed et al. (2011), the anti-correlation between RH and NPEs would simply be due to the fact
428 that solar radiation and photochemistry usually peak at noon when the RH exhibits its lower
429 value. However, in our case, this does not seem to explain the different behavior of RH between

NPE and non-NPE days, since the weather was sunny during the entire field campaign. A possible reason is that the RH was much lower during northwesterly wind periods (Setyan et al., 2012), during which we usually did not observe NPEs.

Fig. 12 shows the average size-resolved mass spectra of organics in 40-120 nm (D_{va}) particles during NPE days and non-event days, along with the mass spectra of biogenic SOA and urban transport SOA reported in Setyan et al. (2012). The average mass spectrum of organics before the growth (i.e., between 8:00 and 10:00) was subtracted in order to remove the influence of particles existing before the start of the growth events. Therefore, the spectra shown in Fig. 12 are the average mass spectra of organic matter that contributed to the growth of 40-120 nm particles between 10:00 – 16:00 during NPE days ($\Delta Org_{40\text{-}120nm}^{NPE}$) and during non-event days ($\Delta Org_{40\text{-}120nm}^{non\text{-}NPE}$), respectively. As shown in Fig. 12a, the spectrum of $\Delta Org_{40\text{-}120nm}^{NPE}$ is dominated by the signal at *m/z* 44 (mostly CO_2^+), while that of *m/z* 43 (mostly $C_2H_3O^+$) is approximately the half of it. The spectrum of $\Delta Org_{40\text{-}120nm}^{NPE}$ is very similar to that of urban transport SOA (r^2 = 0.95; Fig. 12b) but its correlation coefficient towards the spectrum of biogenic SOA is lower (r^2 = 0.87). On the other hand, the spectrum of $\Delta Org_{40\text{-}120nm}^{non\text{-}NPE}$ is very similar to that of biogenic SOA, as shown by the scatterplot of Fig. 12d. We further performed multilinear regression analyses to represent the mass spectra of $\Delta Org_{40\text{-}120nm}^{NPE}$ and $\Delta Org_{40\text{-}120nm}^{non\text{-}NPE}$, respectively, as the linear combinations of the spectra of urban transport SOA and biogenic SOA. Based on this analysis, we estimated that during NPE days, ~ 74% of the organic mass that contributed to the growth of ultrafine particles was SOA formed in urban transport plumes. During non-event days, the growth of ultrafine mode organics, which was much slower compared during NPE, was primarily (~ 76% by mass) due to SOA influenced by regional biogenic emissions.

These results, coupled to the higher concentrations of anthropogenic compounds on NPE days suggest that the growth of new particles in the Sierra Nevada Foothills was mainly driven by anthropogenic precursors transported from Sacramento and that the growth was likely promoted by the interaction between urban plumes and biogenic emissions. These observations may have important implications in our understanding of SOA formation. For example, models used to assess global SOA budget tend to underpredict the SOA concentrations. However, in a

459 recent study, Spracklen et al. (2011) used a model to estimate the global OA source, and
460 compared their results with worldwide AMS observations. When they took into account
461 anthropogenically-controlled biogenic SOA formation in their estimation of the global OA
462 budget, it reduced considerably the bias between their model and AMS observations.
463
464 ## 4 Conclusions
465 New particle growth events were frequently observed during the US DOE's CARES
466 campaign in northern California in June 2010. Presented here is a description of these events
467 observed with two MPSSs deployed at Sacramento (T0, urban site) and Cool (T1, rural site at the
468 Sierra foothills). Our results showed that these growth events took place on a regional scale,
469 predominantly during periods of southwestern flow that transports urban plumes and
470 anthropogenic emissions from the Sacramento metropolitan area and the San Francisco Bay Area
471 near Carquinez Strait. Growth rates were on average higher at T0 (7.1±2.7 nm/hr) than at T1
472 (6.2±2.5 nm/hr), likely due to higher anthropogenic influences at T0. The evolution of the size-
473 resolved chemical composition of these newly formed particles has been investigated in detail
474 with a HR-ToF-AMS deployed at T1. Our results indicate that the new particle growth was
475 mainly driven by organics, with a small contribution of ammonium sulfate. For example, the
476 average increase of the organic mass in ultrafine particles (40-120 nm in D_{va}, which corresponds
477 to 30-85 nm in Stokes (volume equivalent) diameter, assuming no internal voids, sphericity = 1,
478 and density = 1.4 g/cm^3) was 0.7 μg/m^3 during this period, approximately 7 times higher than
479 that of sulfate (0.1 μg/m^3). Our results also indicate that amines were enhanced significantly
480 during the new particle growth, suggesting that this class of compounds likely played a role. The
481 size-resolved mass spectra of organics in the size range 40-120 nm (in D_{va}) during the growth
482 events were very similar to the mass spectrum of anthropogenically-influenced SOA from urban
483 plume. In addition, during the NPE days, the concentrations of photo-oxidation products
484 (formaldehyde, acetaldehyde, sum of methacrolein and methyl vinyl ketone) and species
485 representative of urban emissions (e.g., BC, CO, NO_x, HOA, and toluene) were on average 50%
486 higher than during non-event days. These results suggest that the new particle growth events

were mainly driven by the transported urban plumes and that the growth of new particles was enhanced by the interactions between biogenic emissions and transported urban plumes.

Acknowledgements

This research was supported by the U.S. Department of Energy (DOE), the Office of Science (BER), Atmospheric System Research Program, grant No. DE-FG02-11 ER65293, the California Air Resources Board (CARB), Agreement No. 10-305, and the California Agricultural Experiment Station, Project CA-DETX-2102-H.

References

Ahlm, L., Liu, S., Day, D. A., Russell, L. M., Weber, R., Gentner, D. R., Goldstein, A. H., DiGangi, J. P., Henry, S. B., Keutsch, F. N., VandenBoer, T. C., Markovic, M. Z., Murphy, J. G., Ren, X., and Scheller, S.: Formation and growth of ultrafine particles from secondary sources in Bakersfield, California, J. Geophys. Res., 117, D00V08, 10.1029/2011jd017144, 2012.

Allan, J. D., Alfarra, M. R., Bower, K. N., Coe, H., Jayne, J. T., Worsnop, D. R., Aalto, P. P., Kulmala, M., Hyotylainen, T., Cavalli, F., and Laaksonen, A.: Size and composition measurements of background aerosol and new particle growth in a Finnish forest during QUEST 2 using an Aerodyne Aerosol Mass Spectrometer, Atmospheric Chemistry and Physics, 6, 315-327, 10.5194/acp-6-315-2006, 2006.

Almeida, J., Schobesberger, S., Kurten, A., Ortega, I. K., Kupiainen-Maatta, O., Praplan, A. P., Adamov, A., Amorim, A., Bianchi, F., Breitenlechner, M., David, A., Dommen, J., Donahue, N. M., Downard, A., Dunne, E., Duplissy, J., Ehrhart, S., Flagan, R. C., Franchin, A., Guida, R., Hakala, J., Hansel, A., Heinritzi, M., Henschel, H., Jokinen, T., Junninen, H., Kajos, M., Kangasluoma, J., Keskinen, H., Kupc, A., Kurten, T., Kvashin, A. N., Laaksonen, A., Lehtipalo, K., Leiminger, M., Leppa, J., Loukonen, V., Makhmutov, V., Mathot, S., McGrath, M. J., Nieminen, T., Olenius, T., Onnela, A., Petaja, T., Riccobono, F., Riipinen, I., Rissanen, M., Rondo, L., Ruuskanen, T., Santos, F. D., Sarnela, N., Schallhart, S., Schnitzhofer, R., Seinfeld, J. H., Simon, M., Sipila, M., Stozhkov, Y., Stratmann, F., Tome, A., Trostl, J., Tsagkogeorgas, G., Vaattovaara, P., Viisanen, Y., Virtanen, A., Vrtala, A., Wagner, P. E., Weingartner, E., Wex, H., Williamson, C., Wimmer, D., Ye, P. L., Yli-Juuti, T., Carslaw, K. S., Kulmala, M., Curtius, J., Baltensperger, U., Worsnop, D. R., Vehkamaki, H., and Kirkby, J.: Molecular understanding of sulphuric acid-amine particle nucleation in the atmosphere, Nature, 502, 359-363, 10.1038/nature12663, 2013.

Asmi, E., Frey, A., Virkkula, A., Ehn, M., Manninen, H. E., Timonen, H., Tolonen-Kivimaki, O., Aurela, M., Hillamo, R., and Kulmala, M.: Hygroscopicity and chemical composition of Antarctic sub-micrometre aerosol particles and observations of new particle formation, Atmospheric Chemistry and Physics, 10, 4253-4271, 10.5194/acp-10-4253-2010, 2010.

Barsanti, K. C., McMurry, P. H., and Smith, J. N.: The potential contribution of organic salts to new particle growth, Atmospheric Chemistry and Physics, 9, 2949-2957, 2009.

Boy, M., and Kulmala, M.: Nucleation events in the continental boundary layer: Influence of physical and meteorological parameters, Atmospheric Chemistry and Physics, 2, 1-16, 10.5194/acp-2-1-2002, 2002.

Brock, C. A., Trainer, M., Ryerson, T. B., Neuman, J. A., Parrish, D. D., Holloway, J. S., Nicks, D. K., Jr., Frost, G. J., Hübler, G., Fehsenfeld, F. C., Wilson, J. C., Reeves, J. M., Lafleur, B. G., Hilbert, H., Atlas, E. L., Donnelly, S. G., Schauffler, S. M., Stroud, V. R., and Wiedinmyer, C.: Particle growth in urban and industrial plumes in Texas, J. Geophys. Res., 108, 4111, 10.1029/2002jd002746, 2003.

534 Bzdek, B. R., and Johnston, M. V.: New Particle Formation and Growth in the Troposphere,
535 Analytical Chemistry, 82, 7871-7878, 10.1021/ac100856j, 2010.

536 Bzdek, B. R., Zordan, C. A., Luther, G. W., and Johnston, M. V.: Nanoparticle Chemical
537 Composition During New Particle Formation, Aerosol Sci. Technol., 45, 1041-1048,
538 10.1080/02786826.2011.580392, 2011.

539 Bzdek, B. R., Zordan, C. A., Pennington, M. R., Luther, G. W., and Johnston, M. V.:
540 Quantitative Assessment of the Sulfuric Acid Contribution to New Particle Growth,
541 Environmental Science & Technology, 46, 4365-4373, 10.1021/es204556c, 2012.

542 Canagaratna, M. R., Jayne, J. T., Jimenez, J. L., Allan, J. D., Alfarra, M. R., Zhang, Q., Onasch,
543 T. B., Drewnick, F., Coe, H., Middlebrook, A., Delia, A., Williams, L. R., Trimborn, A. M.,
544 Northway, M. J., DeCarlo, P. F., Kolb, C. E., Davidovits, P., and Worsnop, D. R.: Chemical and
545 microphysical characterization of ambient aerosols with the aerodyne aerosol mass spectrometer,
546 Mass Spectrom. Rev., 26, 185-222, 10.1002/mas.20115, 2007.

547 Charron, A., Birmili, W., and Harrison, R. M.: Factors influencing new particle formation at the
548 rural site, Harwell, United Kingdom, J. Geophys. Res., 112, D14210, 10.1029/2007jd008425,
549 2007.

550 Creamean, J. M., Ault, A. P., Ten Hoeve, J. E., Jacobson, M. Z., Roberts, G. C., and Prather, K.
551 A.: Measurements of Aerosol Chemistry during New Particle Formation Events at a Remote
552 Rural Mountain Site, Environmental Science & Technology, 45, 8208-8216, 10.1021/es103692f,
553 2011.

554 de Gouw, J. A., Middlebrook, A. M., Warneke, C., Goldan, P. D., Kuster, W. C., Roberts, J. M.,
555 Fehsenfeld, F. C., Worsnop, D. R., Canagaratna, M. R., Pszenny, A. A. P., Keene, W. C.,
556 Marchewka, M., Bertman, S. B., and Bates, T. S.: Budget of organic carbon in a polluted
557 atmosphere: Results from the New England Air Quality Study in 2002, J. Geophys. Res.-Atmos.,
558 110, D16305, 10.1029/2004jd005623, 2005.

559 DeCarlo, P. F., Kimmel, J. R., Trimborn, A., Northway, M. J., Jayne, J. T., Aiken, A. C., Gonin,
560 M., Fuhrer, K., Horvath, T., Docherty, K. S., Worsnop, D. R., and Jimenez, J. L.: Field-
561 deployable, high-resolution, time-of-flight aerosol mass spectrometer, Analytical Chemistry, 78,
562 8281-8289, 10.1021/ac061249n, 2006.

563 Dillon, M. B., Lamanna, M. S., Schade, G. W., Goldstein, A. H., and Cohen, R. C.: Chemical
564 evolution of the Sacramento urban plume: Transport and oxidation, J. Geophys. Res.-Atmos.,
565 107, 4045, 10.1029/2001jd000969, 2002.

566 Dunn, M. J., Jiménez, J.-L., Baumgardner, D., Castro, T., McMurry, P. H., and Smith, J. N.:
567 Measurements of Mexico City nanoparticle size distributions: Observations of new particle
568 formation and growth, Geophysical Research Letters, 31, L10102, 10.1029/2004gl019483, 2004.

569 Fast, J. D., Gustafson Jr, W. I., Berg, L. K., Shaw, W. J., Pekour, M., Shrivastava, M., Barnard,
570 J. C., Ferrare, R. A., Hostetler, C. A., Hair, J. A., Erickson, M., Jobson, B. T., Flowers, B.,
571 Dubey, M. K., Springston, S., Pierce, R. B., Dolislager, L., Pederson, J., and Zaveri, R. A.:
572 Transport and mixing patterns over Central California during the carbonaceous aerosol and
573 radiative effects study (CARES), Atmospheric Chemistry and Physics, 12, 1759-1783,
574 10.5194/acp-12-1759-2012, 2012.

575 Ge, X., Shaw, S. L., and Zhang, Q.: Toward Understanding Amines and Their Degradation
576 Products from Postcombustion CO2 Capture Processes with Aerosol Mass Spectrometry,
577 Environmental Science & Technology, 48, 5066-5075, 10.1021/es4056966, 2014.

578 Glasius, M., la Cour, A., and Lohse, C.: Fossil and nonfossil carbon in fine particulate matter: A
579 study of five European cities, J. Geophys. Res.-Atmos., 116, D11302, 10.1029/2011jd015646,
580 2011.

581 Guo, H., Wang, D. W., Cheung, K., Ling, Z. H., Chan, C. K., and Yao, X. H.: Observation of
582 aerosol size distribution and new particle formation at a mountain site in subtropical Hong Kong,
583 Atmospheric Chemistry and Physics, 12, 9923-9939, 10.5194/acp-12-9923-2012, 2012.

584 Hamed, A., Joutsensaari, J., Mikkonen, S., Sogacheva, L., Dal Maso, M., Kulmala, M., Cavalli,
585 F., Fuzzi, S., Facchini, M. C., Decesari, S., Mircea, M., Lehtinen, K. E. J., and Laaksonen, A.:
586 Nucleation and growth of new particles in Po Valley, Italy, Atmospheric Chemistry and Physics,
587 7, 355-376, 10.5194/acp-7-355-2007, 2007.

588 Hamed, A., Korhonen, H., Sihto, S. L., Joutsensaari, J., Jarvinen, H., Petaja, T., Arnold, F.,
589 Nieminen, T., Kulmala, M., Smith, J. N., Lehtinen, K. E. J., and Laaksonen, A.: The role of
590 relative humidity in continental new particle formation, J. Geophys. Res.-Atmos., 116, D03202,
591 10.1029/2010jd014186, 2011.

592 Han, Y., Iwamoto, Y., Nakayama, T., Kawamura, K., Hussein, T., and Mochida, M.:
593 Observation of new particle formation over a mid-latitude forest facing the North Pacific,
594 Atmospheric Environment, 64, 77-84, 10.1016/j.atmosenv.2012.09.036, 2013.

595 Jayne, J. T., Leard, D. C., Zhang, X. F., Davidovits, P., Smith, K. A., Kolb, C. E., and Worsnop,
596 D. R.: Development of an aerosol mass spectrometer for size and composition analysis of
597 submicron particles, Aerosol Sci. Technol., 33, 49-70, 10.1080/027868200410840, 2000.

598 Jeong, C. H., Evans, G. J., McGuire, M. L., Chang, R. Y. W., Abbatt, J. P. D., Zeromskiene, K.,
599 Mozurkewich, M., Li, S. M., and Leaitch, A. R.: Particle formation and growth at five rural and
600 urban sites, Atmospheric Chemistry and Physics, 10, 7979-7995, 10.5194/acp-10-7979-2010,
601 2010.

602 Jimenez, J. L., Canagaratna, M. R., Donahue, N. M., Prevot, A. S. H., Zhang, Q., Kroll, J. H.,
603 DeCarlo, P. F., Allan, J. D., Coe, H., Ng, N. L., Aiken, A. C., Docherty, K. S., Ulbrich, I. M.,
604 Grieshop, A. P., Robinson, A. L., Duplissy, J., Smith, J. D., Wilson, K. R., Lanz, V. A., Hueglin,

C., Sun, Y. L., Tian, J., Laaksonen, A., Raatikainen, T., Rautiainen, J., Vaattovaara, P., Ehn, M., Kulmala, M., Tomlinson, J. M., Collins, D. R., Cubison, M. J., Dunlea, E. J., Huffman, J. A., Onasch, T. B., Alfarra, M. R., Williams, P. I., Bower, K., Kondo, Y., Schneider, J., Drewnick, F., Borrmann, S., Weimer, S., Demerjian, K., Salcedo, D., Cottrell, L., Griffin, R., Takami, A., Miyoshi, T., Hatakeyama, S., Shimono, A., Sun, J. Y., Zhang, Y. M., Dzepina, K., Kimmel, J. R., Sueper, D., Jayne, J. T., Herndon, S. C., Trimborn, A. M., Williams, L. R., Wood, E. C., Middlebrook, A. M., Kolb, C. E., Baltensperger, U., and Worsnop, D. R.: Evolution of Organic Aerosols in the Atmosphere, Science, 326, 1525-1529, 10.1126/science.1180353, 2009.

Jokinen, T., Sipilä, M., Junninen, H., Ehn, M., Lönn, G., Hakala, J., Petäjä, T., Mauldin Iii, R. L., Kulmala, M., and Worsnop, D. R.: Atmospheric sulphuric acid and neutral cluster measurements using CI-APi-TOF, Atmospheric Chemistry and Physics, 12, 4117-4125, 10.5194/acp-12-4117-2012, 2012.

Kerminen, V. M., Paramonov, M., Anttila, T., Riipinen, I., Fountoukis, C., Korhonen, H., Asmi, E., Laakso, L., Lihavainen, H., Swietlicki, E., Svenningsson, B., Asmi, A., Pandis, S. N., Kulmala, M., and Petäjä, T.: Cloud condensation nuclei production associated with atmospheric nucleation: a synthesis based on existing literature and new results, Atmospheric Chemistry and Physics, 12, 12037-12059, 10.5194/acp-12-12037-2012, 2012.

Kleinman, L. I., Springston, S. R., Daum, P. H., Lee, Y. N., Nunnermacker, L. J., Senum, G. I., Wang, J., Weinstein-Lloyd, J., Alexander, M. L., Hubbe, J., Ortega, J., Canagaratna, M. R., and Jayne, J.: The time evolution of aerosol composition over the Mexico City plateau, Atmospheric Chemistry and Physics, 8, 1559-1575, 10.5194/acp-8-1559-2008, 2008.

Komppula, M., Lihavainen, H., Hatakka, J., Paatero, J., Aalto, P., Kulmala, M., and Viisanen, Y.: Observations of new particle formation and size distributions at two different heights and surroundings in subarctic area in northern Finland, J. Geophys. Res., 108, 4295, 10.1029/2002jd002939, 2003.

Koponen, I. K., Virkkula, A., Hillamo, R., Kerminen, V.-M., and Kulmala, M.: Number size distributions and concentrations of the continental summer aerosols in Queen Maud Land, Antarctica, J. Geophys. Res., 108, 4587, 10.1029/2003jd003614, 2003.

Kulmala, M., Kontkanen, J., Junninen, H., Lehtipalo, K., Manninen, H. E., Nieminen, T., Petäjä, T., Sipilä, M., Schobesberger, S., Rantala, P., Franchin, A., Jokinen, T., Järvinen, E., Äijälä, M., Kangasluoma, J., Hakala, J., Aalto, P. P., Paasonen, P., Mikkilä, J., Vanhanen, J., Aalto, J., Hakola, H., Makkonen, U., Ruuskanen, T., Mauldin, R. L., Duplissy, J., Vehkamäki, H., Bäck, J., Kortelainen, A., Riipinen, I., Kurtén, T., Johnston, M. V., Smith, J. N., Ehn, M., Mentel, T. F., Lehtinen, K. E. J., Laaksonen, A., Kerminen, V.-M., and Worsnop, D. R.: Direct Observations of Atmospheric Aerosol Nucleation, Science, 339, 943-946, 10.1126/science.1227385, 2013.

Laaksonen, A., Kulmala, M., O'Dowd, C. D., Joutsensaari, J., Vaattovaara, P., Mikkonen, S., Lehtinen, K. E. J., Sogacheva, L., Dal Maso, M., Aalto, P., Petaja, T., Sogachev, A., Yoon, Y. J.,

642 Lihavainen, H., Nilsson, D., Facchini, M. C., Cavalli, F., Fuzzi, S., Hoffmann, T., Arnold, F.,
643 Hanke, M., Sellegri, K., Umann, B., Junkermann, W., Coe, H., Allan, J. D., Alfarra, M. R.,
644 Worsnop, D. R., Riekkola, M. L., Hyotylainen, T., and Viisanen, Y.: The role of VOC oxidation
645 products in continental new particle formation, Atmospheric Chemistry and Physics, 8, 2657-
646 2665, 2008.

647 Laitinen, T., Ehn, M., Junninen, H., Ruiz-Jimenez, J., Parshintsev, J., Hartonen, K., Riekkola, M.
648 L., Worsnop, D. R., and Kulmala, M.: Characterization of organic compounds in 10-to 50-nm
649 aerosol particles in boreal forest with laser desorption-ionization aerosol mass spectrometer and
650 comparison with other techniques, Atmospheric Environment, 45, 3711-3719,
651 10.1016/j.atmosenv.2011.04.023, 2011.

652 Lehtipalo, K., Sipilä, M., Junninen, H., Ehn, M., Berndt, T., Kajos, M. K., Worsnop, D. R.,
653 Petäjä, T., and Kulmala, M.: Observations of Nano-CN in the Nocturnal Boreal Forest, Aerosol
654 Sci. Technol., 45, 499-509, 10.1080/02786826.2010.547537, 2011.

655 Liu, S., Hu, M., Wu, Z., Wehner, B., Wiedensohler, A., and Cheng, Y.: Aerosol number size
656 distribution and new particle formation at a rural/coastal site in Pearl River Delta (PRD) of
657 China, Atmospheric Environment, 42, 6275-6283, 10.1016/j.atmosenv.2008.01.063, 2008.

658 Lunden, M. M., Black, D. R., McKay, M., Revzan, K. L., Goldstein, A. H., and Brown, N. J.:
659 Characteristics of fine particle growth events observed above a forested ecosystem in the Sierra
660 Nevada Mountains of California, Aerosol Sci. Technol., 40, 373-388,
661 10.1080/02786820600631896, 2006.

662 Makela, J. M., Yli-Koivisto, S., Hiltunen, V., Seidl, W., Swietlicki, E., Teinila, K., Sillanpaa, M.,
663 Koponen, I. K., Paatero, J., Rosman, K., and Hameri, K.: Chemical composition of aerosol
664 during particle formation events in boreal forest, Tellus Ser. B-Chem. Phys. Meteorol., 53, 380-
665 393, 10.1034/j.1600-0889.2001.530405.x, 2001.

666 Modini, R. L., Ristovski, Z. D., Johnson, G. R., He, C., Surawski, N., Morawska, L., Suni, T.,
667 and Kulmala, M.: New particle formation and growth at a remote, sub-tropical coastal location,
668 Atmospheric Chemistry and Physics, 9, 7607-7621, 10.5194/acp-9-7607-2009, 2009.

669 O'Dowd, C. D., Jimenez, J. L., Bahreini, R., Flagan, R. C., Seinfeld, J. H., Hameri, K., Pirjola,
670 L., Kulmala, M., Jennings, S. G., and Hoffmann, T.: Marine aerosol formation from biogenic
671 iodine emissions, Nature, 417, 632-636, 2002.

672 Pierce, J. R., Riipinen, I., Kulmala, M., Ehn, M., Petäjä, T., Junninen, H., Worsnop, D. R., and
673 Donahue, N. M.: Quantification of the volatility of secondary organic compounds in ultrafine
674 particles during nucleation events, Atmospheric Chemistry and Physics, 11, 9019-9036,
675 10.5194/acp-11-9019-2011, 2011.

676 Pierce, J. R., Leaitch, W. R., Liggio, J., Westervelt, D. M., Wainwright, C. D., Abbatt, J. P. D.,
677 Ahlm, L., Al-Basheer, W., Cziczo, D. J., Hayden, K. L., Lee, A. K. Y., Li, S. M., Russell, L. M.,

678 Sjostedt, S. J., Strawbridge, K. B., Travis, M., Vlasenko, A., Wentzell, J. J. B., Wiebe, H. A.,
679 Wong, J. P. S., and Macdonald, A. M.: Nucleation and condensational growth to CCN sizes
680 during a sustained pristine biogenic SOA event in a forested mountain valley, Atmospheric
681 Chemistry and Physics, 12, 3147-3163, 10.5194/acp-12-3147-2012, 2012.

682 Pikridas, M., Riipinen, I., Hildebrandt, L., Kostenidou, E., Manninen, H., Mihalopoulos, N.,
683 Kalivitis, N., Burkhart, J. F., Stohl, A., Kulmala, M., and Pandis, S. N.: New particle formation
684 at a remote site in the eastern Mediterranean, J. Geophys. Res., 117, D12205,
685 10.1029/2012jd017570, 2012.

686 Riipinen, I., Pierce, J. R., Yli-Juuti, T., Nieminen, T., Hakkinen, S., Ehn, M., Junninen, H.,
687 Lehtipalo, K., Petaja, T., Slowik, J., Chang, R., Shantz, N. C., Abbatt, J., Leaitch, W. R.,
688 Kerminen, V. M., Worsnop, D. R., Pandis, S. N., Donahue, N. M., and Kulmala, M.: Organic
689 condensation: a vital link connecting aerosol formation to cloud condensation nuclei (CCN)
690 concentrations, Atmospheric Chemistry and Physics, 11, 3865-3878, 10.5194/acp-11-3865-2011,
691 2011.

692 Riipinen, I., Yli-Juuti, T., Pierce, J. R., Petaja, T., Worsnop, D. R., Kulmala, M., and Donahue,
693 N. M.: The contribution of organics to atmospheric nanoparticle growth, Nature Geoscience, 5,
694 453-458, 10.1038/ngeo1499, 2012.

695 Schichtel, B. A., Malm, W. C., Bench, G., Fallon, S., McDade, C. E., Chow, J. C., and Watson,
696 J. G.: Fossil and contemporary fine particulate carbon fractions at 12 rural and urban sites in the
697 United States, J. Geophys. Res.-Atmos., 113, D02311, 10.1029/2007jd008605, 2008.

698 Setyan, A., Zhang, Q., Merkel, M., Knighton, W. B., Sun, Y., Song, C., Shilling, J. E., Onasch,
699 T. B., Herndon, S. C., Worsnop, D. R., Fast, J. D., Zaveri, R. A., Berg, L. K., Wiedensohler, A.,
700 Flowers, B. A., Dubey, M. K., and Subramanian, R.: Characterization of submicron particles
701 influenced by mixed biogenic and anthropogenic emissions using high-resolution aerosol mass
702 spectrometry: results from CARES, Atmospheric Chemistry and Physics, 12, 8131-8156,
703 10.5194/acp-12-8131-2012, 2012.

704 Shilling, J. E., Zaveri, R. A., Fast, J. D., Kleinman, L., Alexander, M. L., Canagaratna, M. R.,
705 Fortner, E., Hubbe, J. M., Jayne, J. T., Sedlacek, A., Setyan, A., Springston, S., Worsnop, D. R.,
706 and Zhang, Q.: Enhanced SOA formation from mixed anthropogenic and biogenic emissions
707 during the CARES campaign, Atmospheric Chemistry and Physics, 13, 2091-2113, 10.5194/acp-
708 13-2091-2013, 2013.

709 Smith, J. N., Moore, K. F., Eisele, F. L., Voisin, D., Ghimire, A. K., Sakurai, H., and McMurry,
710 P. H.: Chemical composition of atmospheric nanoparticles during nucleation events in Atlanta,
711 Journal of Geophysical Research: Atmospheres, 110, D22S03, 10.1029/2005jd005912, 2005.

712 Smith, J. N., Dunn, M. J., VanReken, T. M., Iida, K., Stolzenburg, M. R., McMurry, P. H., and
713 Huey, L. G.: Chemical composition of atmospheric nanoparticles formed from nucleation in

714 Tecamac, Mexico: evidence for an important role for organic species in nanoparticle growth,
715 Geophysical Research Letters, 35, L04808, 10.1029/2007GL032523, 2008.

716 Smith, J. N., Barsanti, K. C., Friedli, H. R., Ehn, M., Kulmala, M., Collins, D. R., Scheckman, J.
717 H., Williams, B. J., and McMurry, P. H.: Observations of aminium salts in atmospheric
718 nanoparticles and possible climatic implications, Proceedings of the National Academy of
719 Sciences, 107, 6634-6639, 10.1073/pnas.0912127107, 2010.

720 Spracklen, D. V., Carslaw, K. S., Kulmala, M., Kerminen, V. M., Mann, G. W., and Sihto, S. L.:
721 The contribution of boundary layer nucleation events to total particle concentrations on regional
722 and global scales, Atmospheric Chemistry and Physics, 6, 5631-5648, 10.5194/acp-6-5631-2006,
723 2006.

724 Spracklen, D. V., Jimenez, J. L., Carslaw, K. S., Worsnop, D. R., Evans, M. J., Mann, G. W.,
725 Zhang, Q., Canagaratna, M. R., Allan, J., Coe, H., McFiggans, G., Rap, A., and Forster, P.:
726 Aerosol Mass Spectrometer constraint on the global secondary organic aerosol budget, Atmos.
727 Chem. Phys., 11, 12109-12136, 10.5194/acp-11-12109-201, 2011.

728 Stanier, C. O., Khlystov, A. Y., and Pandis, S. N.: Nucleation events during the Pittsburgh air
729 quality study: Description and relation to key meteorological, gas phase, and aerosol parameters,
730 Aerosol Sci. Technol., 38, 253-264, 10.1080/02786820390229570, 2004.

731 Vakkari, V., Laakso, H., Kulmala, M., Laaksonen, A., Mabaso, D., Molefe, M., Kgabi, N., and
732 Laakso, L.: New particle formation events in semi-clean South African savannah, Atmospheric
733 Chemistry and Physics, 11, 3333-3346, 10.5194/acp-11-3333-2011, 2011.

734 Volkamer, R., Jimenez, J. L., San Martini, F., Dzepina, K., Zhang, Q., Salcedo, D., Molina, L.
735 T., Worsnop, D. R., and Molina, M. J.: Secondary organic aerosol formation from anthropogenic
736 air pollution: Rapid and higher than expected, Geophysical Research Letters, 33, L17811,
737 10.1029/2006gl026899, 2006.

738 Weber, R. J., McMurry, P. H., Mauldin, R. L., Tanner, D. J., Eisele, F. L., Clarke, A. D., and
739 Kapustin, V. N.: New Particle Formation in the Remote Troposphere: A Comparison of
740 Observations at Various Sites, Geophysical Research Letters, 26, 307-310,
741 10.1029/1998gl900308, 1999.

742 Wen, J., Zhao, Y., and Wexler, A. S.: Marine particle nucleation: Observation at Bodega Bay,
743 California, J. Geophys. Res., 111, D08207, 10.1029/2005jd006210, 2006.

744 Wiedensohler, A., Birmili, W., Nowak, A., Sonntag, A., Weinhold, K., Merkel, M., Wehner, B.,
745 Tuch, T., Pfeifer, S., Fiebig, M., Fjäraa, A. M., Asmi, E., Sellegri, K., Depuy, R., Venzac, H.,
746 Villani, P., Laj, P., Aalto, P., Ogren, J. A., Swietlicki, E., Williams, P., Roldin, P., Quincey, P.,
747 Hüglin, C., Fierz-Schmidhauser, R., Gysel, M., Weingartner, E., Riccobono, F., Santos, S.,
748 Grüning, C., Faloon, K., Beddows, D., Harrison, R., Monahan, C., Jennings, S. G., O'Dowd, C.
749 D., Marinoni, A., Horn, H. G., Keck, L., Jiang, J., Scheckman, J., McMurry, P. H., Deng, Z.,

750 Zhao, C. S., Moerman, M., Henzing, B., de Leeuw, G., Löschau, G., and Bastian, S.: Mobility
751 particle size spectrometers: harmonization of technical standards and data structure to facilitate
752 high quality long-term observations of atmospheric particle number size distributions,
753 Atmospheric Measurement Techniques, 5, 657-685, 10.5194/amt-5-657-2012, 2012.

754 Wu, Z., Hu, M., Liu, S., Wehner, B., Bauer, S., Ma ßling, A., Wiedensohler, A., Petäjä, T., Dal
755 Maso, M., and Kulmala, M.: New particle formation in Beijing, China: Statistical analysis of a 1-
756 year data set, J. Geophys. Res., 112, D09209, 10.1029/2006jd007406, 2007.

757 Yue, D. L., Hu, M., Zhang, R. Y., Wang, Z. B., Zheng, J., Wu, Z. J., Wiedensohler, A., He, L.
758 Y., Huang, X. F., and Zhu, T.: The roles of sulfuric acid in new particle formation and growth in
759 the mega-city of Beijing, Atmospheric Chemistry and Physics, 10, 4953-4960, 10.5194/acp-10-
760 4953-2010, 2010.

761 Zaveri, R. A., Shaw, W. J., Cziczo, D. J., Schmid, B., Ferrare, R. A., Alexander, M. L.,
762 Alexandrov, M., Alvarez, R. J., Arnott, W. P., Atkinson, D. B., Baidar, S., Banta, R. M.,
763 Barnard, J. C., Beranek, J., Berg, L. K., Brechtel, F., Brewer, W. A., Cahill, J. F., Cairns, B.,
764 Cappa, C. D., Chand, D., China, S., Comstock, J. M., Dubey, M. K., Easter, R. C., Erickson, M.
765 H., Fast, J. D., Floerchinger, C., Flowers, B. A., Fortner, E., Gaffney, J. S., Gilles, M. K.,
766 Gorkowski, K., Gustafson, W. I., Gyawali, M., Hair, J., Hardesty, R. M., Harworth, J. W.,
767 Herndon, S., Hiranuma, N., Hostetler, C., Hubbe, J. M., Jayne, J. T., Jeong, H., Jobson, B. T.,
768 Kassianov, E. I., Kleinman, L. I., Kluzek, C., Knighton, B., Kolesar, K. R., Kuang, C., Kubátová,
769 A., Langford, A. O., Laskin, A., Laulainen, N., Marchbanks, R. D., Mazzoleni, C., Mei, F.,
770 Moffet, R. C., Nelson, D., Obland, M. D., Oetjen, H., Onasch, T. B., Ortega, I., Ottaviani, M.,
771 Pekour, M., Prather, K. A., Radney, J. G., Rogers, R. R., Sandberg, S. P., Sedlacek, A., Senff, C.
772 J., Senum, G., Setyan, A., Shilling, J. E., Shrivastava, M., Song, C., Springston, S. R.,
773 Subramanian, R., Suski, K., Tomlinson, J., Volkamer, R., Wallace, H. W., Wang, J.,
774 Weickmann, A. M., Worsnop, D. R., Yu, X. Y., Zelenyuk, A., and Zhang, Q.: Overview of the
775 2010 Carbonaceous Aerosols and Radiative Effects Study (CARES), Atmospheric Chemistry
776 and Physics, 12, 7647-7687, 10.5194/acp-12-7647-2012, 2012.

777 Zhang, Q., Stanier, C. O., Canagaratna, M. R., Jayne, J. T., Worsnop, D. R., Pandis, S. N., and
778 Jimenez, J. L.: Insights into the chemistry of new particle formation and growth events in
779 Pittsburgh based on aerosol mass spectrometry, Environmental Science & Technology, 38, 4797-
780 4809, 10.1021/es035417u, 2004a.

781 Zhang, Q., Worsnop, D. R., Canagaratna, M. R., and Jimenez, J. L.: Hydrocarbon-like and
782 oxygenated organic aerosols in Pittsburgh: insights into sources and processes of organic
783 aerosols, Atmospheric Chemistry and Physics, 5, 3289-3311, 10.5194/acp-5-3289-2005, 2005.

784 Zhang, Q., Jimenez, J. L., Canagaratna, M. R., Allan, J. D., Coe, H., Ulbrich, I., Alfarra, M. R.,
785 Takami, A., Middlebrook, A. M., Sun, Y. L., Dzepina, K., Dunlea, E., Docherty, K., DeCarlo, P.
786 F., Salcedo, D., Onasch, T., Jayne, J. T., Miyoshi, T., Shimono, A., Hatakeyama, S., Takegawa,
787 N., Kondo, Y., Schneider, J., Drewnick, F., Borrmann, S., Weimer, S., Demerjian, K., Williams,

788 P., Bower, K., Bahreini, R., Cottrell, L., Griffin, R. J., Rautiainen, J., Sun, J. Y., Zhang, Y. M.,
789 and Worsnop, D. R.: Ubiquity and dominance of oxygenated species in organic aerosols in
790 anthropogenically-influenced Northern Hemisphere midlatitudes, Geophysical Research Letters,
791 34, L13801, 10.1029/2007gl029979, 2007.

792 Zhang, X. F., Smith, K. A., Worsnop, D. R., Jimenez, J. L., Jayne, J. T., Kolb, C. E., Morris, J.,
793 and Davidovits, P.: Numerical characterization of particle beam collimation: Part II - Integrated
794 aerodynamic-lens-nozzle system, Aerosol Sci. Technol., 38, 619-638,
795 10.1080/02786820490479833, 2004b.

796 Zhang, Y. M., Zhang, X. Y., Sun, J. Y., Lin, W. L., Gong, S. L., Shen, X. J., and Yang, S.:
797 Characterization of new particle and secondary aerosol formation during summertime in Beijing,
798 China, Tellus Ser. B-Chem. Phys. Meteorol., 63, 382-394, 10.1111/j.1600-0889.2011.00533.x,
799 2011.

800 Ziemba, L. D., Griffin, R. J., Cottrell, L. D., Beckman, P. J., Zhang, Q., Varner, R. K., Sive, B.
801 C., Mao, H., and Talbot, R. W.: Characterization of aerosol associated with enhanced small
802 particle of number concentrations in a suburban forested environment, J. Geophys. Res.-Atmos.,
803 115, D12206, 10.1029/2009jd012614, 2010.

804 Zollner, J. H., Glasoe, W. A., Panta, B., Carlson, K. K., McMurry, P. H., and Hanson, D. R.:
805 Sulfuric acid nucleation: power dependencies, variation with relative humidity, and effect of
806 bases, Atmospheric Chemistry and Physics, 12, 4399-4411, 10.5194/acp-12-4399-2012, 2012.
807
808

809 **Table 1.** Summary of the characteristics of new particle growth events observed at Sacramento
810 (T0) and Cool (T1) in northern California.

Day	T0				T1						
	Growth rate nm/hr	ΔN/Δt #/cm^3/hr	$\Delta N_{12\text{-}20\ nm}$ #/cm^3	NPE Event	Growth rate nm/hr	ΔN/Δt #/cm^3/hr	$\Delta N_{12\text{-}20\ nm}$ #/cm^3	$\Delta Org_{\ 40\text{-}120\ nm}$ µg/m^3/hr	$\Delta SO_4^{2-}{}_{\ 40\text{-}120\ nm}$ µg/m^3/hr	Wind	NPE Event
6/2/2010	Incomplete SMPS data			N/A[a]	Incomplete SMPS data			0.75	0.10	T0→T1[b]	N/A
6/3/2010	10.5	6.12E+03	5.43E+03	strong	4.1	2.56E+03	3.35E+03	0.98	0.32	T0→T1	strong
6/4/2010	5.4	6.80E+03	5.44E+03	strong	12.5	6.14E+03	1.70E+03	Incomplete PToF data		T0→T1	strong
6/5/2010	10.9	9.57E+03	3.77E+03	strong	9.3	1.07E+03	1.10E+03	No PToF data		T0→T1	weak
6/6/2010	12.1	7.40E+03	4.57E+03	strong	8.8	2.98E+03	1.01E+03	Incomplete PToF data		T0→T1	weak
6/7/2010	10.1	6.40E+03	4.83E+03	strong	7.6	5.86E+03	1.51E+03	0.28	0.063	T0→T1	strong
6/8/2010	4.1	5.64E+03	4.28E+03	strong	7.7	4.19E+03	2.63E+03	0.35	0.075	T0→T1	strong
6/9/2010	7.3	1.21E+04	1.18E+04	strong	6.1	6.92E+03	4.86E+03	0.49	0.075	T0→T1	strong
6/10/2010	6.5	7.76E+03	1.44E+03	weak	4.2	4.31E+03	1.33E+03	0.19	0.0	NW	weak
6/11/2010	7.1	2.48E+03	1.16E+03	weak	-[c]	-	-	-	-	NW	no NPG
6/12/2010	-	-	-	no NPG	Incomplete data					NW	N/A
6/13/2010	-	-	-	no NPG	-	-	-	-	-	NW	no NPG
6/14/2010	4.6	1.26E+04	8.67E+03	strong	Incomplete data					T0→T1	N/A
6/15/2010	4.4	6.75E+03	8.81E+03	strong	3.8	4.52E+03	3.29E+03	0.27	0.095	T0→T1	strong
6/16/2010	2.5	4.50E+03	6.55E+03	strong	3.6	1.59E+03	1.35E+03	-	-	NW	weak
6/17/2010	-	-	-	no NPG	2.9	2.28E+03	8.08E+02	0.19	0.0	NW	weak
6/18/2010	6.7	3.56E+04	8.25E+03	strong	4.3	5.30E+03	1.74E+03	0.32	0.032	T0→T1	strong
6/19/2010	3.4	2.60E+04	9.55E+03	strong	5.9	5.20E+03	1.48E+03	0.19	0.041	T0→T1	weak
6/20/2010	4.1	8.69E+03	6.02E+03	strong	4.4	2.04E+03	8.86E+02	-	-	NW	weak
6/21/2010	5.2	4.19E+03	1.25E+03	weak	9.5	1.96E+03	9.89E+02	0.17	0.0	NW	weak
6/22/2010	7.6	1.51E+04	5.03E+03	strong	Incomplete SMPS data			0.10	0.0	T0→T1	N/A
6/23/2010	11.1	7.28E+03	1.45E+03	weak	Incomplete SMPS data			0.17	0.060	T0→T1	N/A
6/24/2010	6.4	7.11E+03	8.74E+03	strong	7.6	8.28E+03	2.27E+03	0.64	0.13	T0→T1	strong
6/25/2010	8.0	4.07E+03	4.16E+03	strong	4.7	3.15E+03	9.77E+02	0.31	0.0	T0→T1	weak
6/26/2010	7.7	9.13E+03	6.93E+03	strong	5.3	1.81E+03	8.26E+02	0.27	0.11	T0→T1	weak
6/27/2010	9.3	5.25E+03	6.70E+03	strong	5.6	1.34E+03	1.01E+03	0.11	0.0	T0→T1	weak
6/28/2010				undefined[d]				-	-	T0→T1	undefined
mean	7.1	9.57E+03	5.67E+03		6.2	3.76E+03	1.74E+03	0.34	0.06		
std dev	2.7	7.62E+03	2.90E+03		2.5	2.09E+03	1.09E+03	0.24	0.08		
median	6.9	7.20E+03	5.44E+03		5.6	3.15E+03	1.35E+03	0.27	0.06		
min	2.5	2.48E+03	1.16E+03		2.9	1.07E+03	8.08E+02	0.10	0.0		
max	12.1	3.56E+04	1.18E+04		12.5	8.28E+03	4.86E+03	0.98	0.32		

811 [a] "N/A" stands for not applicable
812 [b] "T0 → T1" stands for T0 to T1 transport periods
813 [c] "-" means that no increase was observed
814 [d] "undefined" means that the MPSS data did not allow to determine whether a growth event took
815 place or not, because of a change in the wind direction during the day.

816 **Table 2.** Summary of average value ± 1 standard deviation for meteorological parameters,
817 particle phase species, and gaseous species during new particle event (NPE) and non-NPE days
818 at the T1 site between 8:00 and 18:00 PDT.

Parameter	NPE days	Non-NPE days
Meteorological data		
Temperature (^{o}C)	24.2 ± 4.4	25.0 ± 4.1
Relative humidity (%)	45.3 ± 12.6	27.1 ± 12.1
Solar radiation (W m^{-2})	702.9 ± 246.1	792.7 ± 200.4
Particle phase		
Particle number (# cm^{-3})	9.4E3 ± 6.1E3	4.1E3 ± 1.9E3
Growth rate (nm/hr)	6.2 ± 2.5	-
Biogenic SOA (μg m^{-3})	0.90 ± 0.65	0.56 ± 0.27
Urban transport SOA (μg m^{-3})	1.2 ± 0.90	0.54 ± 0.44
HOA (μg m^{-3})	0.16 ± 0.15	0.11 ± 0.08
SO_4^{2-} (μg m^{-3})	0.39 ± 0.22	0.14 ± 0.10
NO_3^- (μg m^{-3})	0.13 ± 0.08	0.054 ± 0.036
BC (μg m^{-3})	0.042 ± 0.028	0.027 ± 0.017
Trace gases (ppb)		
Terpenes	0.058 ± 0.088	0.043 ± 0.034
Isoprene	1.40 ± 1.02	1.35 ± 0.80
MACR + MVK	0.98 ± 0.79	0.75 ± 0.50
Methanol	6.36 ± 3.12	5.36 ± 1.76
Acetone	1.90 ± 1.09	1.64 ± 0.42
Formaldehyde	2.71 ± 1.39	1.83 ± 0.81
Acetaldehyde	0.97 ± 0.47	0.71 ± 0.24
Acetic acid	0.98 ± 1.10	0.87 ± 0.43
Acetonitrile	0.18 ± 0.03	0.17 ± 0.02
Benzene	0.036 ± 0.029	0.031 ± 0.014
Toluene	0.060 ± 0.037	0.038 ± 0.019
O_3	43.5 ± 14.2	46.2 ± 10.5
NO_x	3.8 ± 3.3	2.7 ± 3.5
CO	130.1 ± 27.0	99.8 ± 19.8

819

Figure 1. Time series of (a, d) wind direction colored by wind speed, (b, e) broadband solar radiation, temperature and relative humidity, and (c, f) particle size distributions at the T0 and T1 sites.

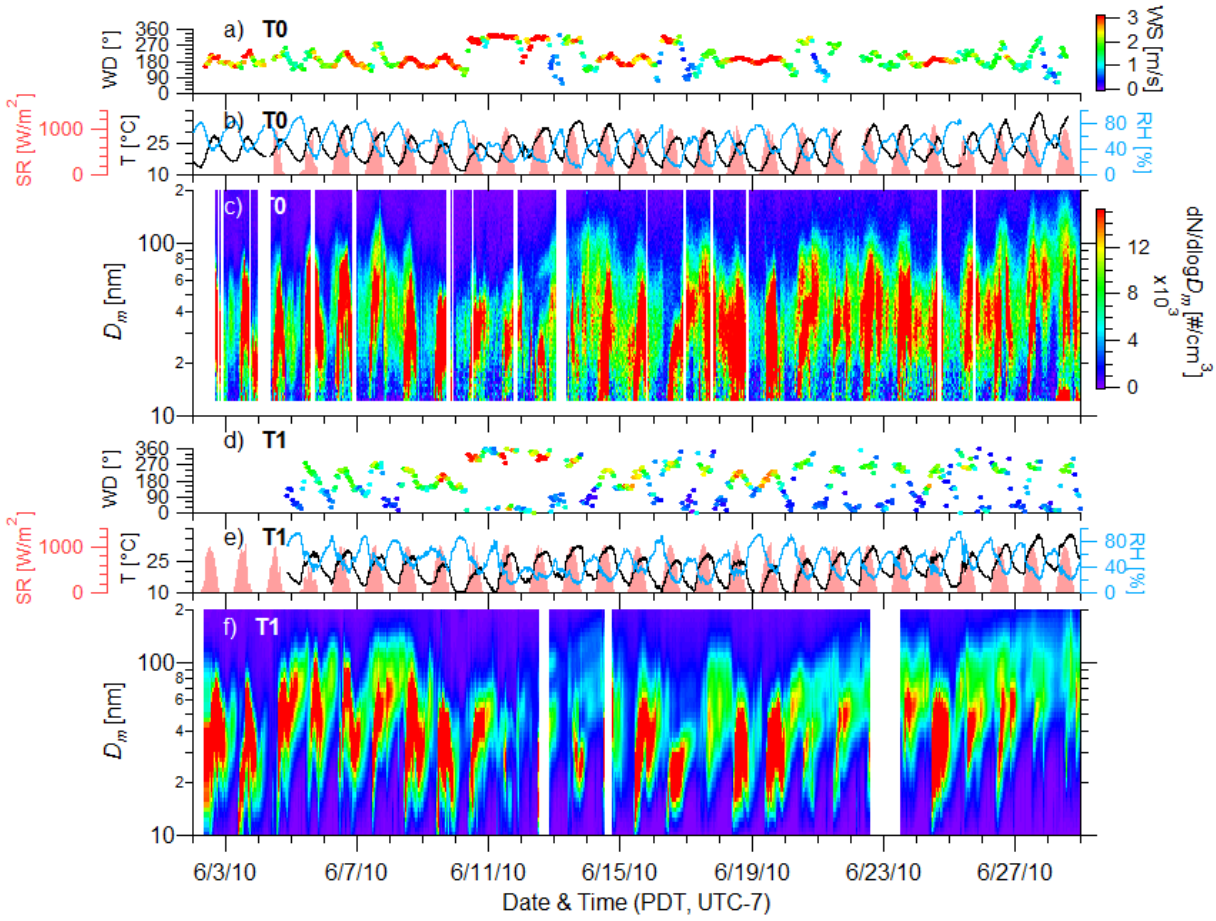

824 **Figure 2.** Diurnal patterns of particle number concentrations measured at the T0 and T1 sites
825 during NPE days.

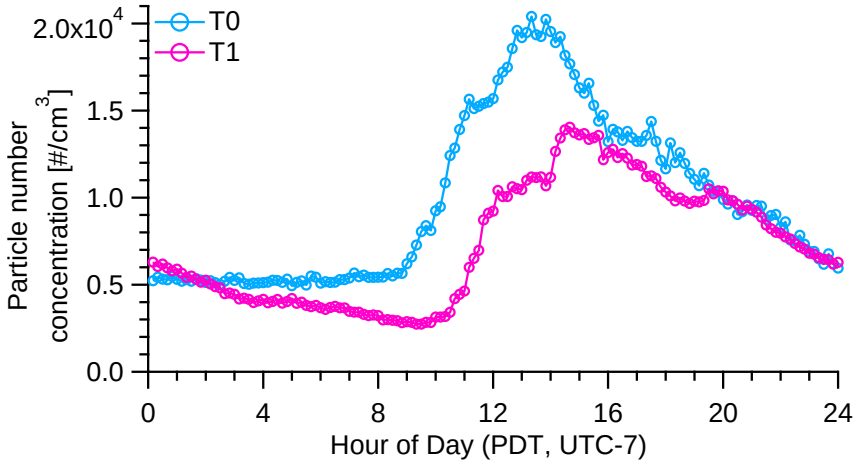

826

Figure 3. Comparison of the time evolution of the particle size distributions at the (a) T0 and (b) T1 sites on June 26, along with the hourly averaged wind direction (length of the arrows is proportional to the wind speed) for each site. Time series of (c) NR-PM_1 species and BC, and (d) three different OA factors.

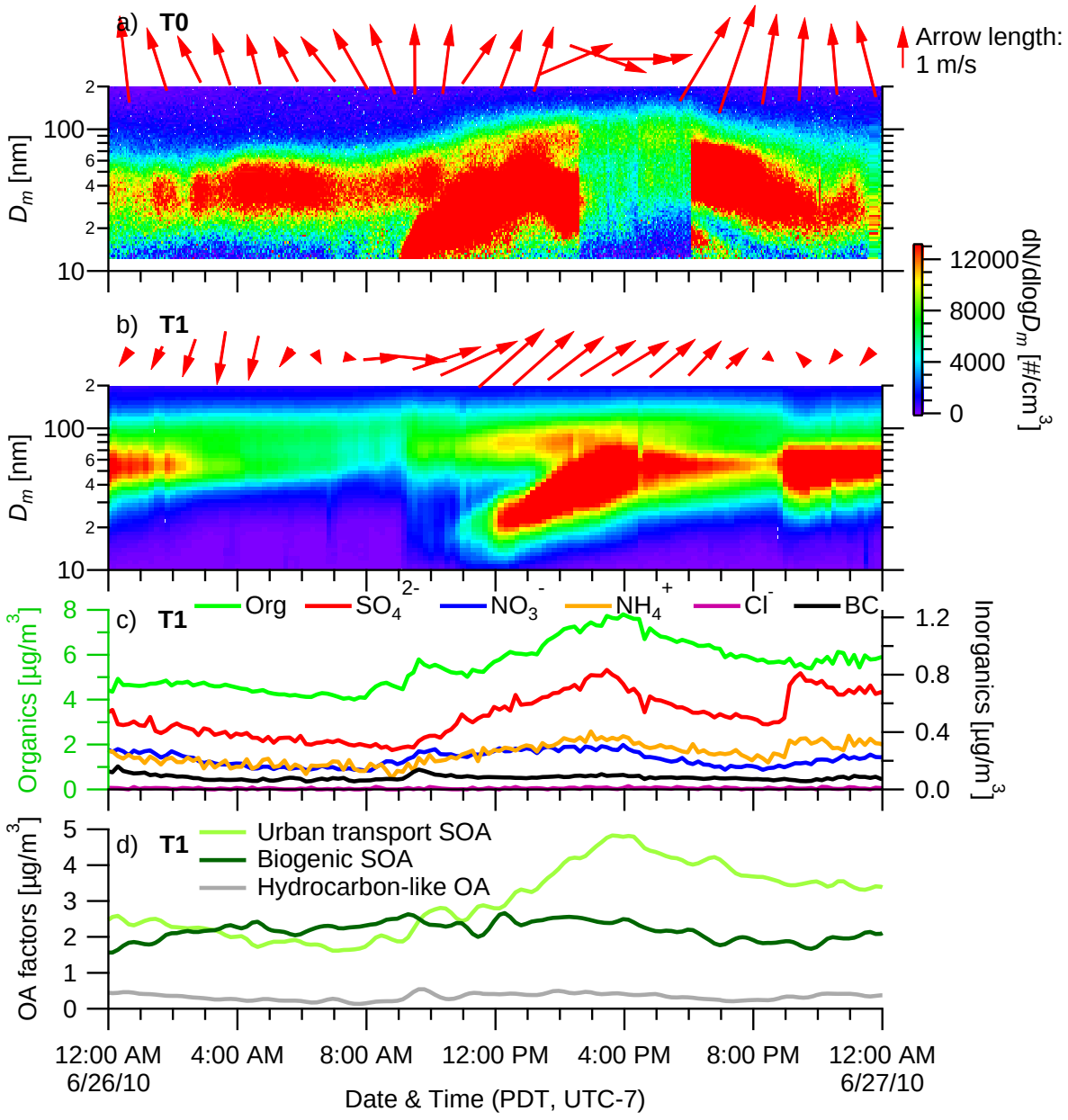

Figure 4. Comparisons of the average particle number size distributions for each hour at T0 and T1 during June 26.

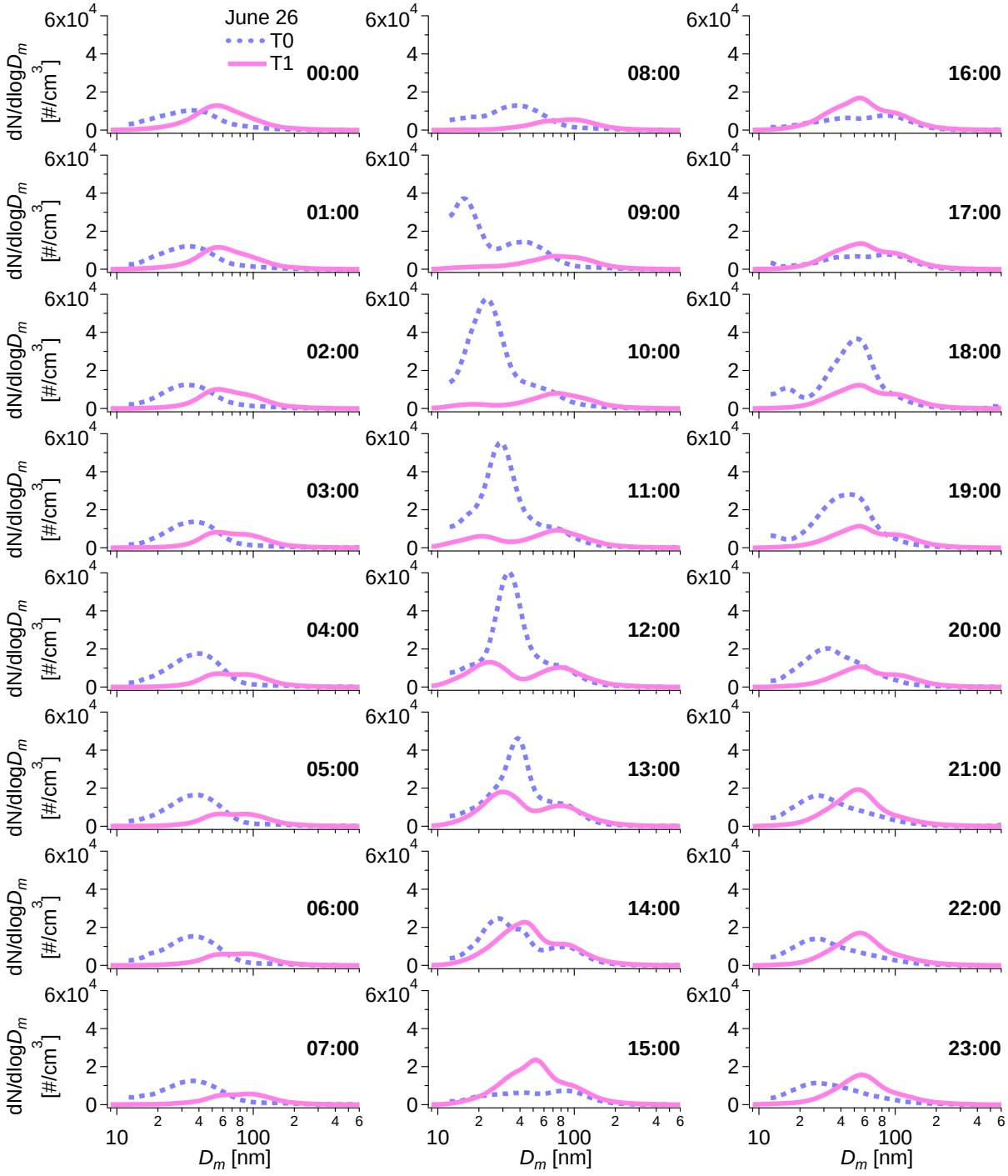

Figure 5. Diurnal size distributions of the particle number concentration at the (a, b) T0 and (c, d) T1 sites during NPE days (left panel) and non-NPE days (right panel). Black crosses correspond to the modal diameters fitted by log-normal distributions.

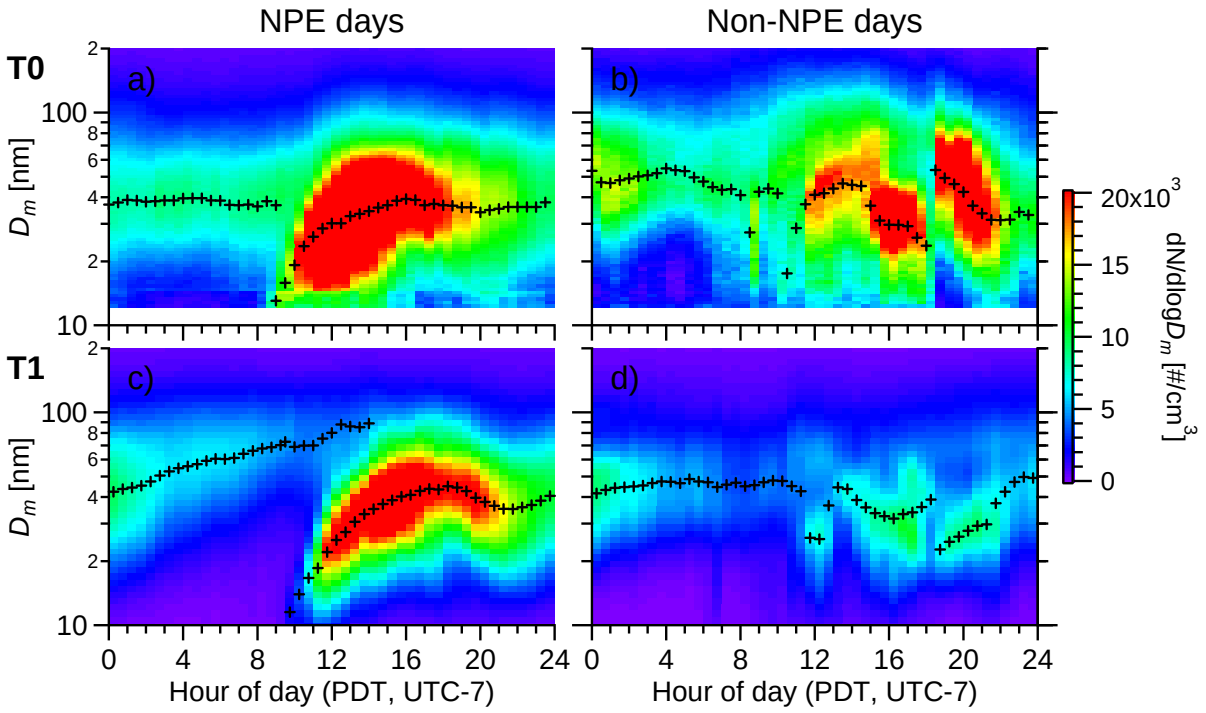

Figure 6. Diurnal size distributions of (a, b) Org, (c, d) SO_4^{2-}, and (e, f) particle volume concentrations, and (g, h) daytime wind rose plots (8:00-20:00 PDT) for NPE days (left panel) and non-NPE days (right panel).

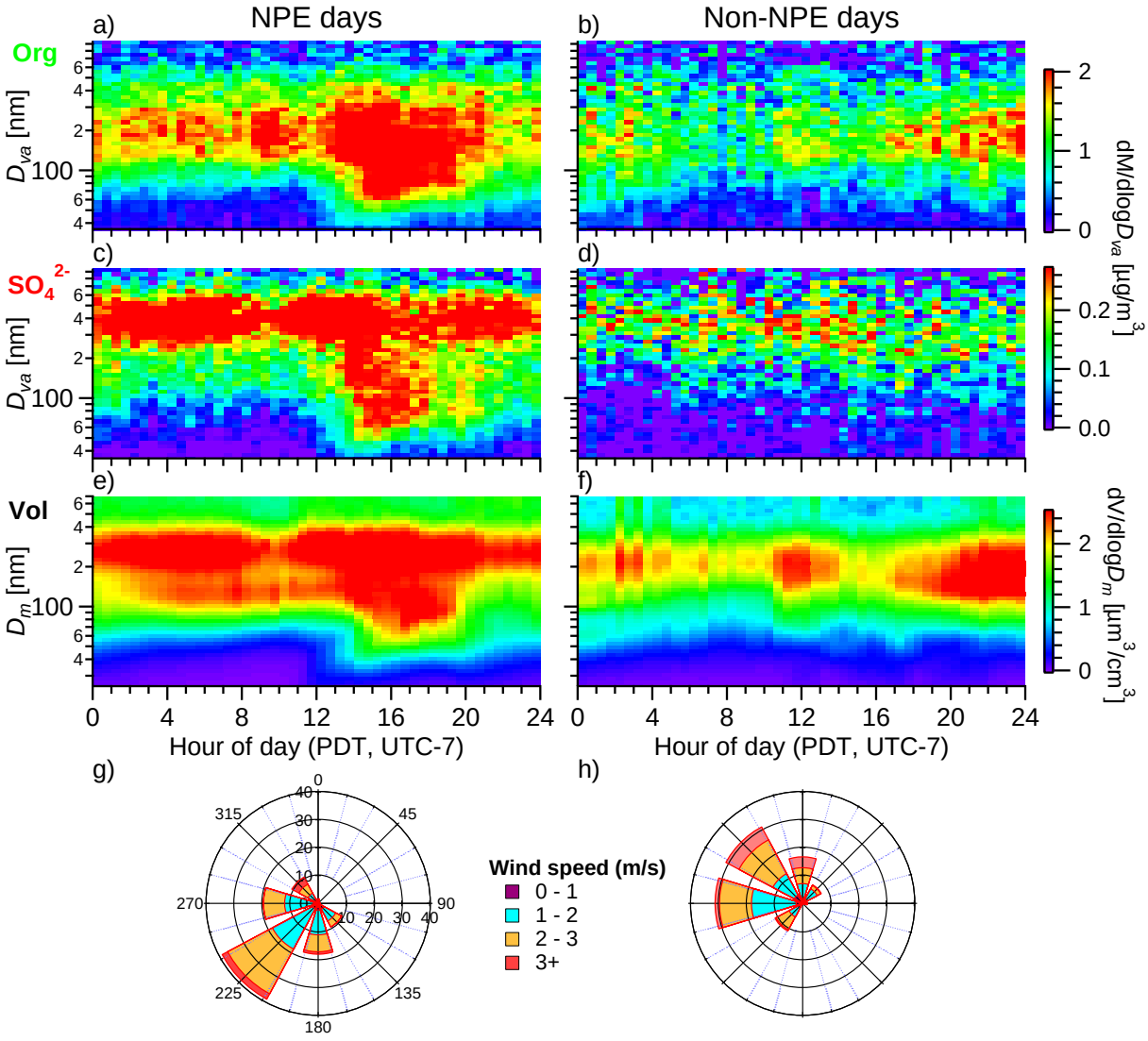

Figure 7. Diurnal patterns of the concentrations of (a, b) Org and (c, d) SO_4^{2-} (black circles and lines, right y-axes) and the mass fractions in the range 40-120, 120-200 and 200-800 nm (in D_{va}, left y-axes) during NPE days (left panel) and non-NPE days (right panel).

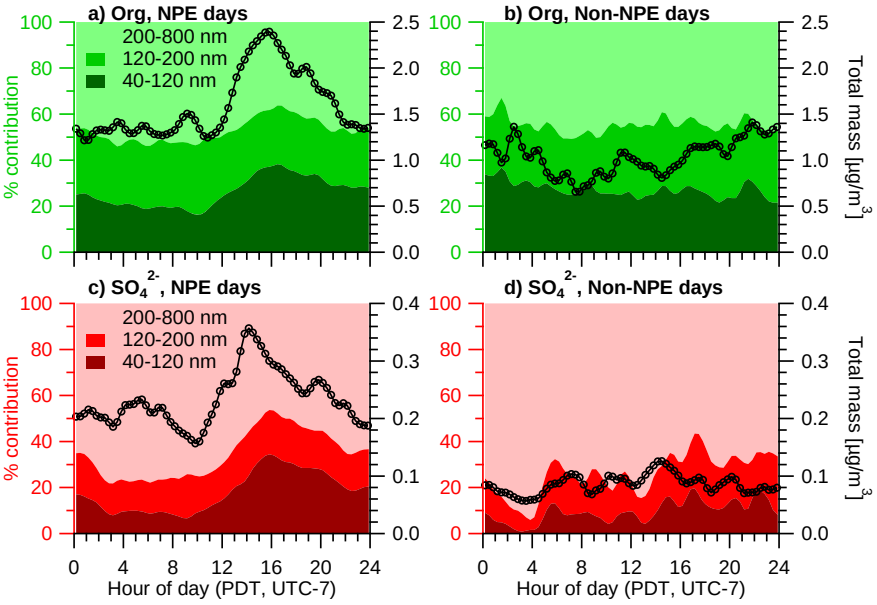

Figure 8. Diurnal patterns of (a) particle number concentration (10-15 nm), (b) urban transport SOA, (c) biogenic SOA, (d) SO_4^{2-} (40-120 nm in D_{va}), (e) Org (40-120 nm in D_{va}), and (f) N-containing organic ions (= CHN^+ + CH_4N^+ + $C_2H_3N^+$ + $C_2H_4N^+$) and ammonium during NPE (solid symbols) and non-NPE (open symbols) days.

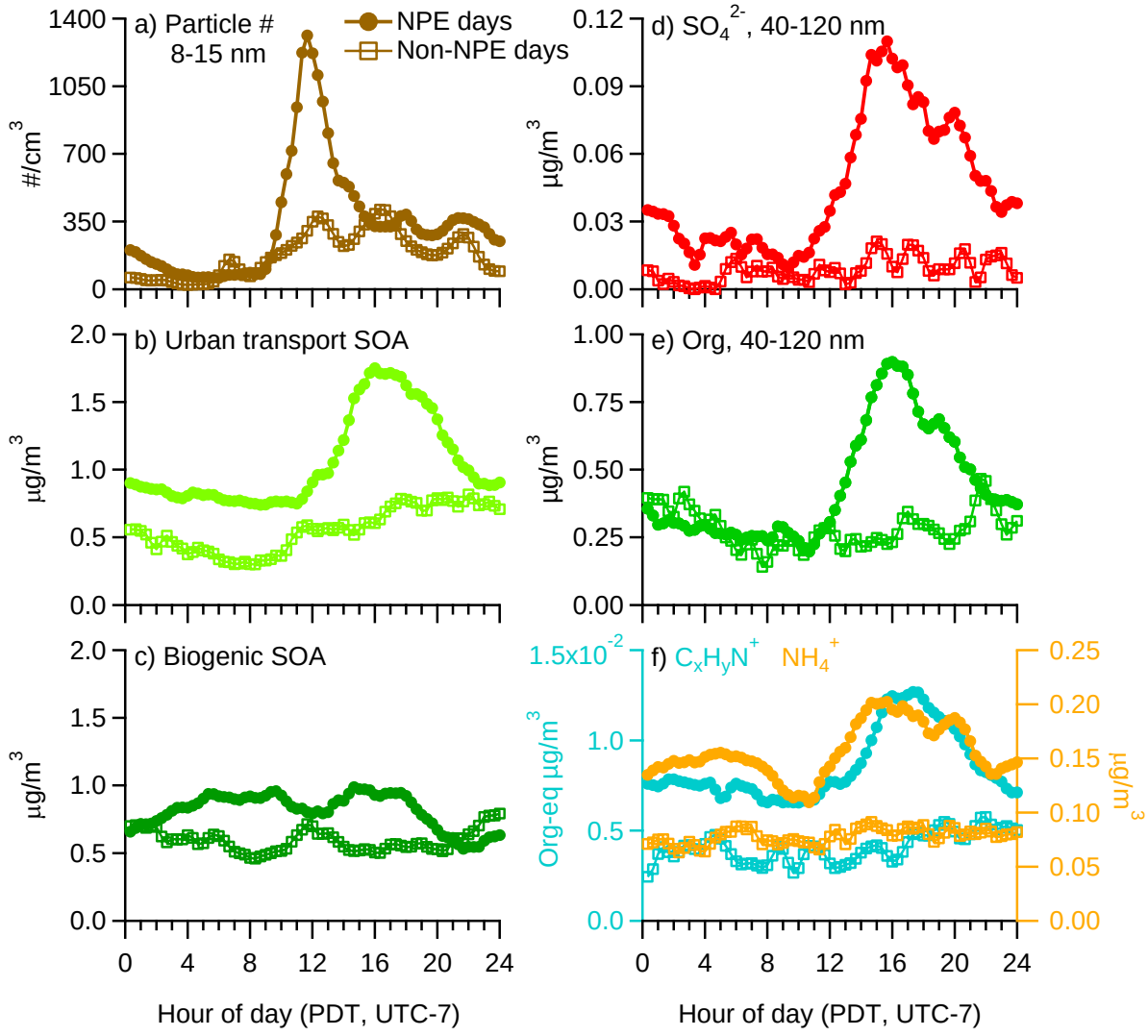

Figure 9. 2-hour averaged size distributions of (a, b) particle number and (c, d) volume, (e, f) SO_4^{2-}, and (g, h) Org during NPE days (left panel) and non-NPE days (right panel) between 8:00 and 18:00 (PDT).

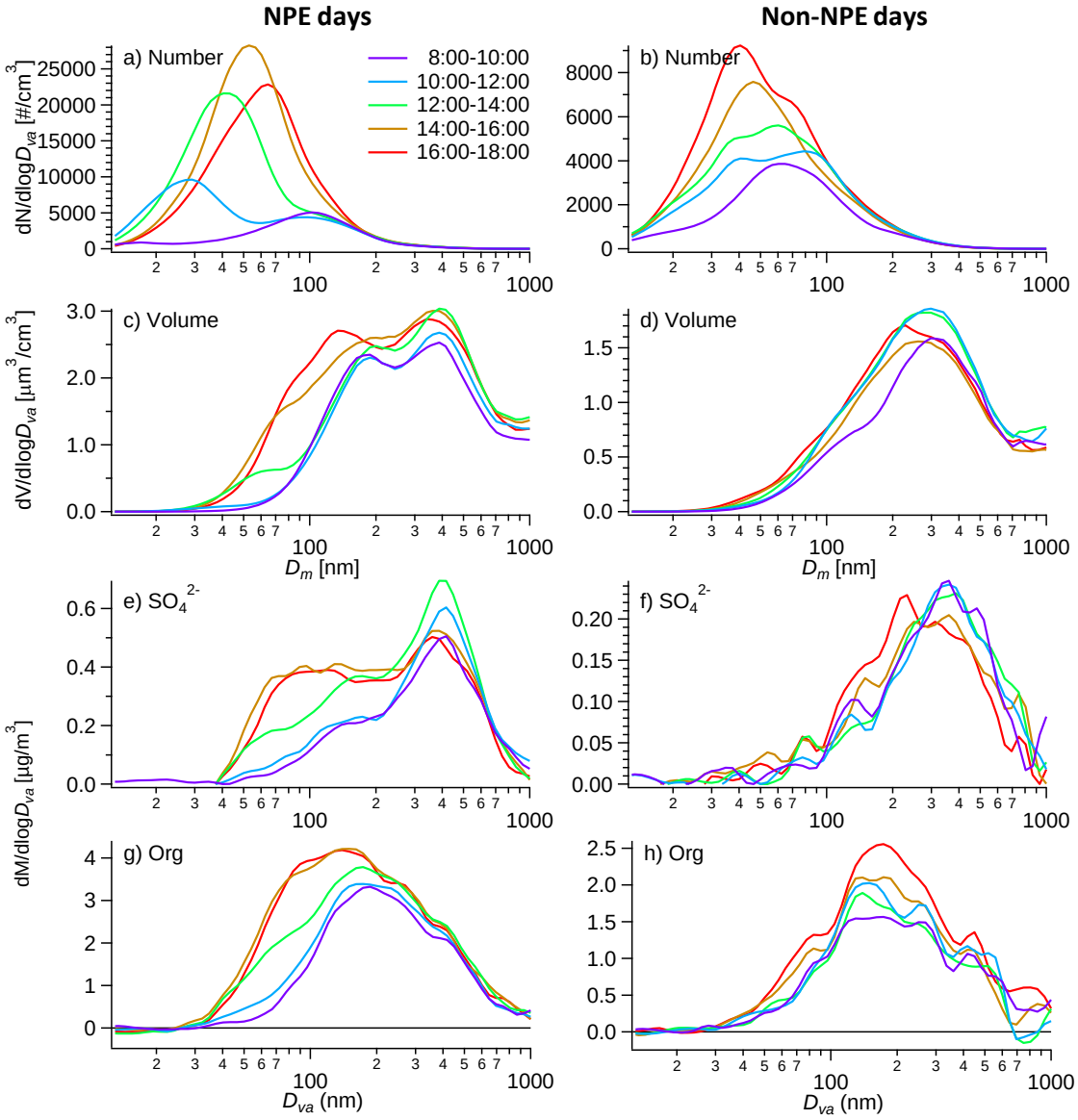

Figure 10. Size distributions of SO_4^{2-}, NH_4^+ and the ratio of measured NH_4^+ to predicted NH_4^+ (= $2 \cdot SO_4^{2-} \cdot 18/96$) between (a) 10:00-11:00, (b) 14:00-15:00, and (c) 18:00-19:00 during NPE days.

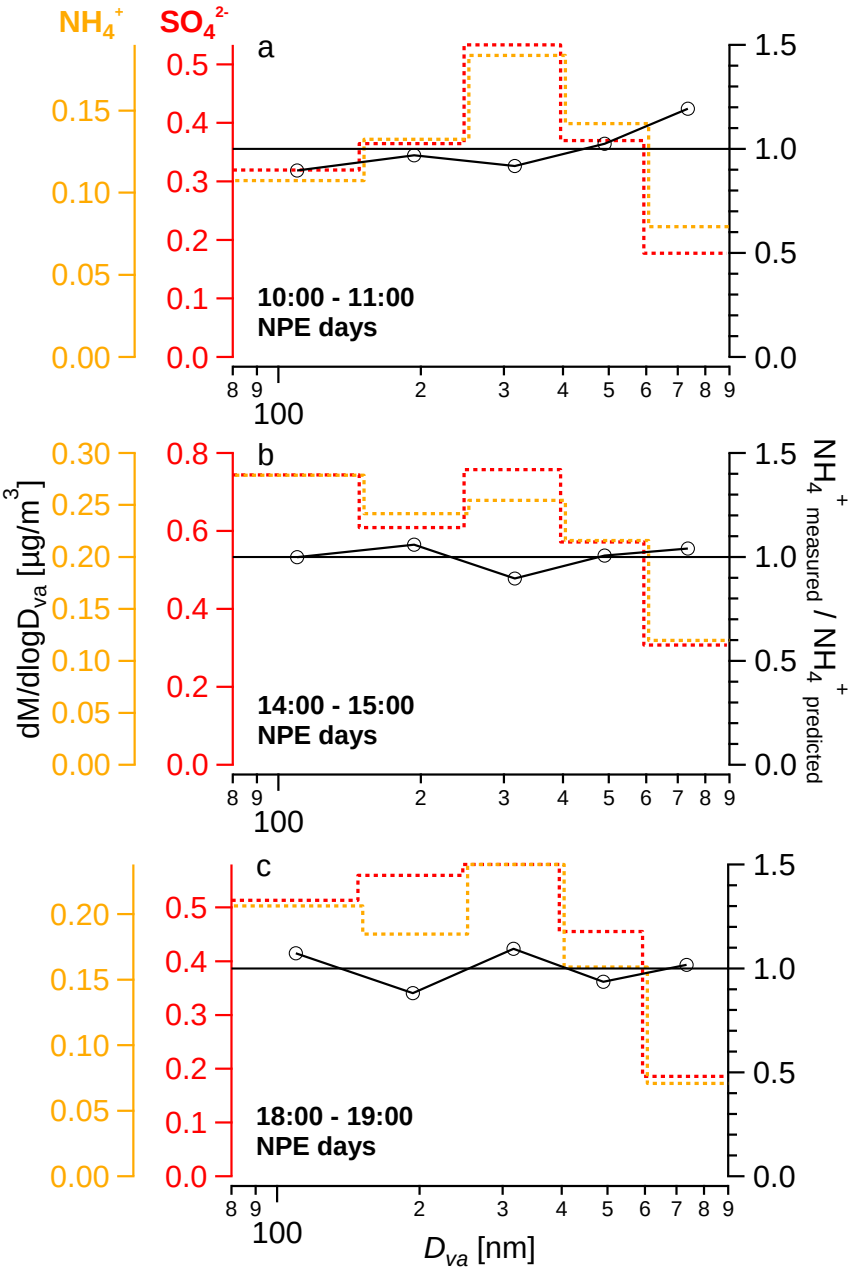

Figure 11. (b) Average concentrations of VOCs, O_3, NO_x, CO, BC, NR-PM_1 species, different OA factors, and N-containing organic ions (= CHN^+ + CH_4N^+ + $C_2H_3N^+$ + $C_2H_4N^+$) between 8:00 and 18:00 (PDT) during NPE and non-NPE days. (a) NPE days / Non-NPE days ratios for the same parameters.

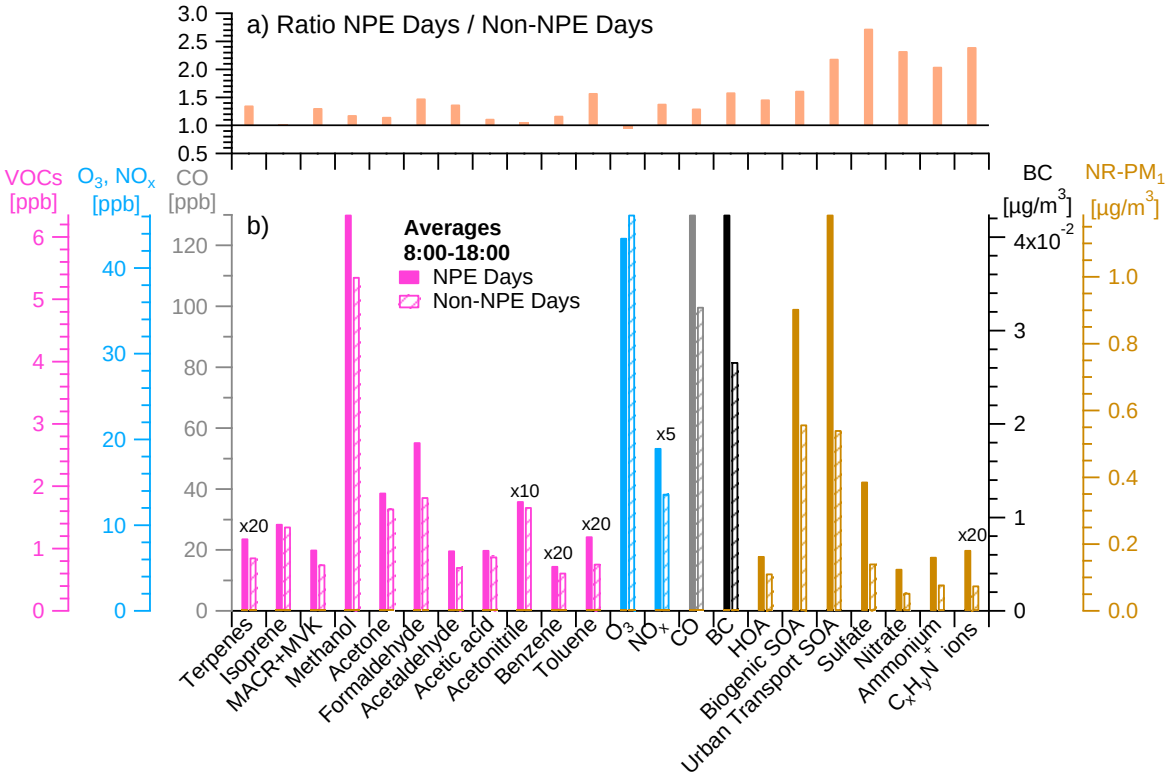

Figure 12. Average mass spectra of (a) urban transport SOA and $\Delta Org_{40\text{-}120nm}$ (i.e., organics that contribute to the growth of 40-120 nm particles) during NPE days, and (c) biogenic SOA and $\Delta Org_{40\text{-}120nm}$ during Non-NPE days. Scatterplots that compare the mass spectra of (b) urban transport SOA vs. $\Delta Org_{40\text{-}120nm}$ during NPE days, and (d) biogenic SOA vs. $\Delta Org_{40\text{-}120nm}$ during non-NPE days. The data fitting of these two scatterplots was performed using the orthogonal distance regression (ODR).